

FF

CERN-TIS-99-008-TE

su. 5831

EUROPEAN ORGANIZATION FOR NUCLEAR RESEARCH

CERN - TIS - 99-008 - TE

April 1999

HIGH-LEVEL DOSIMETRY RESULTS FOR THE CERN HIGH-ENERGY ACCELERATORS

Part 1: PS complex 1998

A. Fontaine and M. Tavlet

Abstract

This year again, the high-level dosimetry results are presented in three separate reports: this one concerns the doses in the machines and tunnels of the PS complex, Part 2 concerns the doses in the SPS complex and Part 3, the doses in the LEP machine. The results are presented in the form of graphs and are discussed separately for each area. The aim of this report is to provide a dose estimate for the components of the various accelerators, and to draw attention to possible radiation damage.

CERN LIBRARIES, GENEVA



SCAN-9908028

1. INTRODUCTION

Integrated radiation dose measurements at selected points in high-dose-level areas give reliable information on radiation ageing of accelerator materials, and provide an indication of their projected lifetime. The small radiation detectors allow the actual received dose to be sensed near the exposed component. We do not, however, keep track of the movement and exchange of equipment, although this needs to be taken into account for the determination of the total integrated doses of individual components.

These measurements have been carried out at the PS since 1966 [1] and at the PS Booster since 1975 [2]. The accelerators LIL (LEP Injector Linacs) and EPA (Electron-Positron Accumulator) are included in the programme as from 1987 onwards. The new ISOLDE area was equipped with dosimeters in May 1992 and the transfer line Booster - ISOLDE in February 1993. The Compact Linear Collider (CLIC) started in 1996 and was also equipped with dosimeters.

The SPS machine and its related target areas and transfer lines were included at the start of operation in 1976 [3]. The LEP machine and transfer tunnels were equipped with dosimeters in 1989 [4].

In addition to dose measurements in the standard positions, some more dosimeters were measured for users of PS, SPS, LEP and experiments in 1998. The dosimeters of the special cable position in the PS were not read this year.

Since a few years, the cameras have also been included in the programme.

The standard dosimeter positions in the different areas are given in Table 1 and Fig. 1. Most of the dosimeters for which the results are presented in this report were read during the annual shutdown.

This report gives the integrated dose values for the year 1998 as well as the integrated doses from the start of the machines.

The values measured earlier can be found in Refs. [5] and [6].

2. DOSIMETRY METHODS

Three types of standard dosimeters are used for high-dose measurements :

- Radio-photo-luminescent (RPL) glass dosimeters;
- Hydrogen-pressure dosimeters (HPD);
- Polymer-alanine dosimeters (PAD).

In proton machines and tunnels such as the PS complex, mainly RPL dosimeters are used. Electrons liberated in glass during irradiation may be trapped in vacancies or by impurities, forming more or less stable colour centres of different types. In silver-doped

RPL glass the luminescent orange light, which is emitted after excitation by UV light, is evaluated to obtain the irradiation dose [7].

For the HPD the pressure of hydrogen, released by irradiated polyethylene, is measured by means of a small vacuum chamber and a pressure-sensor device; this pressure is about proportional to the absorbed dose up to 10 MGy [8].

Stable free radicals are created in alanine by ionizing radiation. The unpaired electron comes from the breaking of a carbon covalent bond, and is detected by the electron spin resonance (ESR) technique. Although a sophisticated readout apparatus is required, ESR spectroscopy has the advantage that a high precision and stability can be reached [9, 10].

The dosimeters are calibrated with a ^{60}Co source. This means that all doses reported here are those that would be needed in order to produce the same signal, by a ^{60}Co gamma irradiation, in a $(\text{CH}_2)_n$ -type material. These dosimetry methods are sufficiently reliable, as can be seen from dosimeter-comparison experiments carried out in accelerator radiation environments, and from our experience of radiation damage in plastic materials. Some parameters and the range of application for these dosimeters are listed in Table 1 of HS-RP/060, in Ref. [6]; further details may be found in Refs.[7 - 12]. In order to investigate their behaviour at cryogenic temperatures, RPL and PAD dosimeters have been irradiated at 77 K and 4.5 K. The results are published in Refs. [13] and [14].

3. RESULTS

As in the preceding reports (Refs. [5] and [6]), the results presented here are in the form of graphs as summarised in the attached figures (Figs. 2-17). The graphs either present the dose records for the year 1998, or the total integrated doses from the beginning of the dose record up to the end of the year 1998. Critical dose limits above which radiation damage to accelerator components could occur can be set at the following levels:

- 10^2 Gy for electronic components;
- 10^5 to 10^6 Gy for organic cable-insulating materials;
- 10^7 to 10^8 Gy for magnet coil insulations.

Although we have placed over 2000 dosimeters in the surveyed areas (of which 592 in the PS complex), the record given above is far from being complete and must be used as a general indication only.

For instance, the radiation-sensitive item of concern is not necessarily located at or close to the spot where the dosimeter is positioned. For locations further away from the radiation source, the dose may be estimated by applying a $1/r^{1.25}$ distance factor.

The results presented in the graphs are self-explanatory. A few additional comments are given below for each accelerator. If no dose is plotted in a particular position, then the dosimeter was lost.

Statistical data about PS accelerators operation were taken from Ref. [15].

3.1. PS Booster

Table 2 shows the summation over the 106 dosimeter readings, which is proportional to the total irradiation doses per ring, and the summation over the four rings, since 1975.

The number of protons for each ring is missing for 1990, 1991, and 1992 because these data were not given in the statistics of the PS operation.

Table 3 gives the evolution of the integrated doses per accelerated proton (IAP) and of the average intensity of the beams.

The integrated doses along the injection lines and around the PSB ring for 1998 and for the years 1975 to 1998, are shown in Figs. 2a and 2b.

Appendix 1 at the end of this report explains the magnet positions which correspond to the nomenclature in the PSB (from IR/86-31, in Ref. [6]).

In 1998, doses of more than or about 1 MGy were measured in positions 57 on rings 1, 2 and 3 (BR1, BR2 and BR3.BHZ82U), in position 59 on ring 4 (BR4.BHZ91U) and in position 75 on ring 3 (BR3.BHZ112U). In 1998, 10 positions on Ring 3 absorbed a dose higher than 1.10^5 Gy compared to 11 in 1997. The comparison of the yearly doses graphs for the years 96, 97 and 98 show changes in the global aspect, the positions 59, 69 on ring 3 are no more 'peak points' in 1998 (diminution of more than a factor 10 for position 69). They are replaced by positions 57 on ring 3 and 59 on ring 4 with annual doses of more than 2 MGy.

Figures 3 to 5 show the evolution of different parameters such as number of accelerated protons, total integrated dose, integrated dose per accelerated proton (IAP) and average beam intensity. They use the results from Table 2 and 3.

In 1998, these parameters show an inverted tendency compared to 1997: reduction of the number of accelerated protons, increase of realised time, increase of ~30% of the total integrated dose. This leads to an increase of the IAP and a decrease of the average intensity

The distribution of doses recorded from 1975 to 1998 at 95 magnet coils of ring 3 in the PSB is shown in Fig. 6. The data used for these summary representations are taken from Fig. 2b but only concern the ring 3. It is to be noted that insulation failure might start to happen on magnet coils having absorbed more than 10 MGy.

3.2. ISOLDE areas

Figure 7a shows the integrated doses in the transfer line between the Booster and the ISOLDE target area for the year 1998 and Fig. 7b the integrated doses from 1993 to 1998. Absorbed doses in the ISOLDE target area are shown in Fig. 8a for 1998, and the integrated doses from 1992 to 1998 in Fig. 8b.

In the Booster-ISOLDE transfer line, doses are in general higher in 1998 than in 1997. On magnet BTY-BVT101, the dose increase is the most important, upstream as well as downstream. Upstream, the dose increases by a factor 5 and goes again above 1 MGy.

Downstream, the multiplication factor reaches 20 with an absorbed dose of $3.3 \cdot 10^5$ Gy. It is to be noted that this evolution takes place after important reductions in 1997. The magnets QDE-120 and QDE-151 also kept about the same level of integrated dose. In other positions, the increases from 1997 to 1998 concern really low dose levels. In the ISOLDE target area, the doses (point to point) are in general lower than in 1997 excepted in some positions where the increase is remarkable (from factor 4 to 24), e.g. on MTV 321 and downstream of magnet QFO 322.

3.3. PS main ring

Integrated doses over 100 straight sections in standard positions are given in Fig. 9a for the year 1998 and in Fig. 9b for the period between 1966 and 1998.

In 1998, six straight-section positions showed doses significantly higher than 10^5 Gy, namely 37, 39, 43 (as in 1997) 34, 35 and 63.

The integrated dose per accelerated proton (IAP) stayed stable compared to 1997, the yearly dose variation being compensated by the higher number of accelerated protons. (Table 4 and Fig.10).

The distribution of absorbed doses recorded at these 100 positions is shown in Fig. 11 for the period 1966 to 1998.

3.4. LIL target area

Figure 12a shows the doses for 1998 and Figure 12b the integrated doses from 1987 to 1998 in the target area.

The yearly doses are lower than in 1997 except on BHZ22 where the dose has more than doubled in one year but remaining still low for this area.

3.5. CLIC Test Facility

Figure 13a shows the absorbed doses in 1998 and Figure 13b the integrated doses from 1996. In 1998, the BHZ-E-152 was surrounded by shielding blocks. The dose mentioned on the graph is the dose absorbed by a dosimeter placed above the blocks. An other dosimeter was glued on the backside of the blocks, it absorbed 29 Gy.

In 1997, the dosimeter placed directly on the BHZ-E-152 has absorbed 2 kGy.

3.6. Doses on TV cameras

Integrated doses on TV cameras which are located at the Booster, LPI, LINAC, LEAR, TT2, AA, ISOLDE II, and the East zone of PS were measured in 1998. The results can be found in Figs. 14 to 17.

References

1. K. Goebel and M. Nielsen, Routine flux density and dose-rate measurements near the PS vacuum chamber, CERN HP-69-69 Rev. (1969)
2. M. Chanel, Mesures d'irradiation au PSB, CERN PS/BR Note 76-18 (1976)
3. F. Coninckx and H. Schönbacher, Doses to the SPS from 1976 to 1986 and estimate of radiation damage, Nucl. Instrum. & Methods A288 (1990)
4. F. Coninckx, Dosimétrie à haut niveau dans le LEP. TIS-CFM/TM/89-10F.
5. P. Bossard et al., Radiation dose measurements around the CERN high-energy accelerators PSB, PS and SPS, HS-RP/023 (1978), plus Add. 1 (1978) and Add. 2 (1979).
6. F. Coninckx et al., High-level dosimetry results for the CERN high-energy accelerators, HS-RP/060 (1981), HS-RP/IR/82-41/Rev.(1982), TIS-RP/IR/83-51, /84-43, /85-30, /86-31, /202 (1987), /210 (1988), TIS-CFM/89-08, /90-22, /91-10, /92-10, /93-11, /94-11, /95-12, /96-09, and TIS-TE/97-21, 98-07.
7. K. Becker, Solid-state dosimetry. CRC Press, Cleveland (1973)
8. J.T. Morgan, R. Sheldon, G.B. Stapleton and G. Wilkinson, A continuous reading and a single measurement dosimeter for the range 10^4 - 10^9 rad, RPP/E14, Rutherford High Energy Laboratory (April 1980).
9. F. Coninckx et al., Alanine dosimetry as reference dosimetric system in accelerator radiation environment, TIS-CFM/216/CF (1988), Appl. Radiat. & Isot. **40**, (1989) 977.
10. F. Coninckx and H. Schönbacher, Experience with a new polymer-alanine dosimeter in a high energy particle accelerator environment, CERN-TIS-CFM/IR 91-13 (1991), and Appl. Radiat. & Isot. **44**, No.1/2 (1993) 67.
11. F. Coninckx et al., Comparison of high-dose dosimetry systems for radiation damage studies in collider detectors and accelerators, CERN/TIS-CFM/92-12/PP (1992); Nucl. Instrum. & Methods in Phys. Res. B **83** (1993) 181-188.
12. E. Florian, H. Schönbacher and M. Tavlet, Data compilation of dosimetry methods and radiation sources for material testing, CERN/TIS-CFM/IR/93-03 (1993).
13. F. Coninckx et al.: Response of Radio-Photo-Luminescent dosimeters irradiated at cryogenic temperatures, CERN/TIS-CFM/95-08 (1995), Radiat. Prot. Dosim. **66**, No. 1-4 (1996) pp. 205-208.
14. F. Coninckx et al.: Response of Alanine dosimeters to irradiations at cryogenic temperatures, CERN/TIS-CFM/95-09/CF (1995), Appl. Radiat. Isot. **47**, No 11/12 (1996) pp. 1223-1229.
15. D. Dagan, Operation Statistics of the PS accelerator complex for 1998, PS/OP/Note 98-45 and on the network : div_ps on Srv1_home.

Table captions

1. Location of RPL dosimeters in the PS and Booster (PSB).
2. Total integrated doses in the PSB and the corresponding numbers of accelerated protons.
3. Average intensity and doses per accelerated proton in the PSB.
4. Accelerated protons and yearly doses integrated over 100 straight sections of the PS.

Figure captions

Fig. 1. Position of the dosimeters in the PSB and in the PS.

Distance of the dosimeters from the beam line axis: PSB: 3 cm; PS: 3.5 cm.

Fig. 2a. PS Booster integrated doses for 1998.

Full line = Ring 3 (■). Others symbols show particular points in Ring 1 (u), Ring 2 (●) and Ring 4 (s). The horizontal scale shows the dosimeter location in the injection line, the periods 1 to 16 and the transfer line. For an explanation of the numbers, see Appendix 1 at the end of the report. Number of accelerated protons in 1998: 13.01×10^{19} .

Fig. 2b. PS Booster integrated doses from 1975 to 1998.

Symbol as in Fig. 2a. Integrated number of accelerated protons: 20.24×10^{20} .

Fig. 3. Total absorbed dose and number of accelerated protons evolution over 4 rings from 1975 to 1998 in the PSB.

Fig. 4. Average intensity and dose per accelerated proton evolution over 4 rings from 1975 to 1998 in the PSB.

Fig. 5. Integrated dose per accelerated proton in the PSB: evolution and comparison for the 4 rings from 1975 to 1998.

Fig. 6. Graph of dose-range distribution to the PSB for the period 1975 to 1998.

The measured values used for this summary representation are shown in Fig. 2b (Ring 3).

Fig. 7a. Integrated doses in the transfer line Booster – ISOLDE in 1998.

Fig. 7b. Integrated doses in the transfer line Booster – ISOLDE from 1993 to 1998.

Fig. 8a. Integrated doses in ISOLDE target area in 1998.

Fig. 8b. Integrated doses in ISOLDE target area from February 1992 to November 1998.

Fig. 9a. PS integrated doses in 1998 in straight sections 1 to 100. Number of accelerated protons in 1998: 3.89×10^{19} .

Fig. 9b. PS integrated doses from July 1966 to November 1998 in straight sections 1 to 100. Number of accelerated protons in this period: 14.86×10^{20} .

Fig. 10. Total absorbed dose and integrated dose per accelerated proton (IAP) evolution over 100 straight sections in the PS from 1966 to 1998.

Fig. 11. Graph of dose-range distribution to the PS from 1966 to 1998. The measured values used for this representation are shown in Fig. 9b.

Fig. 12a. Integrated doses in the target area of LIL from April to November 1998.

Fig. 12b. Integrated doses in the target area of LIL from 1987 to 1998.

Fig. 13a. Integrated doses in the CLIC Test Facility from April to November 1998.

Fig. 13b. Integrated doses in the CLIC Test Facility from October 1996 to November 1998.

Fig. 14 to 17. Integrated doses on TV cameras for 1998 in the Booster, LPI, LINAC, LEAR, TT, AA, ISOLDE II, and the East zone of the PS.

Appendix

1. Nomenclature of the positions in the PS-Booster.

Table 1. Location of RPL dosimeters in the PS complex

Machine	Area	Location	Results
PS Booster	Injection Linac-Booster Transfer Booster-PS	On vacuum chamber upstream of the magnet.	
	Ring 3: Rings 1, 2, 4: period 1, 2 (injection 50 MeV) period 6 (reference) period 9 (beamscope) period 9 (targets) period 15, 16 (ejection,int. dump)	On vacuum chamber upstream and downstream of bending magnets, and upstream of quadrupoles.	Figs. 2a and 2b
	Transfer Booster-Isolde	On vacuum chamber up and downstream magnet. On TV cameras.	Figs. 7a and 7b Fig. 14
	Isolde target area	On vacuum chamber up and downstream magnet. On target caissons. On TV cameras.	Figs. 8a and 8b Fig. 17
PS	100 straight sections sections 5, 21, 42, 55 and 93	Downstream of each magnet unit on the vacuum chamber. On cables.	Figs. 9a and 9b
LIL	Linac and production target	Vacuum chamber and around production target.	Figs. 12a and 12b
EPA	Around the accumulator	Up and downstream magnets and septa. On TV cameras	Fig. 14
LINAC		On TV cameras	Fig. 15
LEAR		On TV cameras	Fig. 15
Clic Test Facility		On various components On TV cameras	Figs. 13a and 13b Fig. 14
AA	Production target	On TV cameras New positions to be identified	Fig. 16

Table 2

Total integrated doses in the PSB and
the corresponding numbers of accelerated protons

Year		Ring	1	2	3	4	Total	
1975	6500 h		1.1	2.2	2.2	1	6.5	$\times 10^6$ Gy
			0.6	0.6	0.7	0.6	2.5	$\times 10^{19}$ protons
1976 - 1978	19000 h		13.6	22.3	21.3	14.3	71.5	$\times 10^6$ Gy
			4.77	4.89	5.01	4.91	19.58	$\times 10^{19}$ protons
1979 - 1981	18000 h		8.04	16.61	15.58	11	51.23	$\times 10^6$ Gy
			4.92	5.62	5.91	5.8	22.25	$\times 10^{19}$ protons
1982	6500 h		1.06	2.09	3.09	2.82	9.06	$\times 10^6$ Gy
			2.23	2.22	2.56	2.45	9.46	$\times 10^{19}$ protons
1983	6500 h		1.6	4.55	2.18	3.79	12.12	$\times 10^6$ Gy
			2.35	2.83	2.73	2.28	10.19	$\times 10^{19}$ protons
1984	6270 h		0.93	5.41	12	1.41	19.75	$\times 10^6$ Gy
			1.3	4.48	4.48	1.3	11.56	$\times 10^{19}$ protons
1985	6474 h		0.27	3.57	15.9	0.76	20.5	$\times 10^6$ Gy
			0.57	5.03	4.82	0.57	10.99	$\times 10^{19}$ protons
1986	6380 h		0.17	0.74	10	0.36	11.27	$\times 10^6$ Gy
			0.87	3.49	3.26	0.72	8.34	$\times 10^{19}$ protons
1987	4374 h		0.79	0.62	1.29	1.26	3.96	$\times 10^6$ Gy
			0.7	1.22	1.08	0.65	3.65	$\times 10^{19}$ protons
1988	6262 h		2.59	2.11	1.88	0.84	7.42	$\times 10^6$ Gy
			1.05	2.92	1.99	0.73	6.69	$\times 10^{19}$ protons
1989	6479 h		0.37	0.53	1	0.53	2.43	$\times 10^6$ Gy
			0.98	2.32	2.49	1.09	6.88	$\times 10^{19}$ protons
1990	6584 h		0.76	0.63	0.79	1.02	3.20	$\times 10^6$ Gy
							5.37	$\times 10^{19}$ protons
1991 - 1992	12465 h		0.57	0.31	1.04	0.57	2.49	$\times 10^6$ Gy
							10.73	$\times 10^{19}$ protons
1993	5861 h		0.16	0.23	1.01	0.38	1.79	$\times 10^6$ Gy
			2.58	2.66	2.56	2.72	10.52	$\times 10^{19}$ protons
1994	5728 h		0.47	0.8	1.21	2.09	4.57	$\times 10^6$ Gy
			2.77	2.79	2.62	2.68	10.86	$\times 10^{19}$ protons
1995	6378 h		4.73	4.48	2.67	3.77	15.65	$\times 10^6$ Gy
			2.64	3.42	3.43	2.86	12.35	$\times 10^{19}$ protons
1996	6582 h		3.38	11.49	4.77	2.74	22.37	$\times 10^6$ Gy
			3.35	3.55	3.36	3.33	13.59	$\times 10^{19}$ protons
1997	6166 h		2.38	3.11	5.73	3.1	14.32	$\times 10^6$ Gy
			3.25	3.67	3.58	3.4	13.904	$\times 10^{19}$ protons
1998	6503 h		2.22	3.95	6.03	6.07	18.26	$\times 10^6$ Gy
			3.06	3.37	3.28	3.30	13.01	$\times 10^{19}$ protons
Total from 1975 to 1998		149006 h	45.19	85.73	109.67	57.81	298.39	$\times 10^6$ Gy
							202.42	$\times 10^{19}$ protons

Table 3

Average intensity and doses per accelerated proton in the PSB
summed over 424 measuring points

(For total dose values see Table 2.)

Year	No of accelerated protons ($\times 10^{19}$)	Average intensity ($\text{p/h} \times 10^{16}$)	IAP (Gy per accelerated proton $\times 10^{-12}$)
1975	2.5	0.39	0.26
1976	5.66	0.65	0.3
1977	5.22	1.3	0.56
1978	8.7	1.38	0.3
1979-1980	16.15	1.66	0.21
1981	6.1	0.73	0.28
1982	9.46	1.46	0.1
1983	10.19	1.55	0.12
1984	11.56	1.84	0.17
1985	10.99	1.7	0.19
1986	8.34	1.31	0.14
1987	3.65	0.83	0.11
1988	6.68	1.07	0.11
1989	6.88	1.06	0.04
1990	5.37	0.82	0.06
1991-1992	10.73	0.86	0.02
1993	10.52	1.79	0.02
1994	10.86	1.9	0.04
1995	12.35	1.94	0.13
1996	13.59	2.06	0.16
1997	13.9	2.25	0.1
1998	13.01	2	0.14
Total 1966 - 1998	202.4	1.359	0.15

Table 4

Accelerated protons and yearly doses
integrated over 100 straight sections of the PS

Year	No of accelerated protons $\times 10^{19}$	Dose to PS (Gy, $\times 10^7$)	IAP (Gy per accelerated proton, $\times 10^{-12}$)
1966	0.5	1.32	2.63
1967	0.64	1.1	1.71
1968	0.45	1.44	3.23
1969	1.08	2.92	2.69
1970	1.1	2.98	2.7
1971	1.25	3.41	2.73
1972	1.14	2.95	2.6
1973	1.45	2.67	1.84
1974	1.77	2.14	1.21
1975	2.27	2.33	1.02
1976	2.8	2.77	0.99
1977	3.66	1.82	0.5
1978	6.42	1.88	0.29
1979	7.26	3.98	0.54
1980	6.03	1.9	0.32
1981	5.27	1.34	0.25
1982	8.51	1.12	0.13
1983	9.68	0.26	0.03
1984	10.93	0.41	0.04
1985	9.79	0.42	0.04
1986	7.15	0.42	0.06
1987	2.56	0.3	0.12
1988	6.07	0.27	0.05
1989	6.27	0.23	0.04
1990	5.47	0.2	0.04
1991	4.75	0.18	0.04
1992	4.18	0.2	0.05
1993	5.59	0.22	0.04
1994	5.51	0.26	0.05
1995	5.73	0.3	0.05
1996	5.83	0.37	0.06
1997	3.63	0.29	0.08
1998	3.89	0.30	0.08
Total 1966 - 1998	148.63	46.44	0.31

STANDARD DOSIMETER POSITION IN THE PS AND IN THE BOOSTER

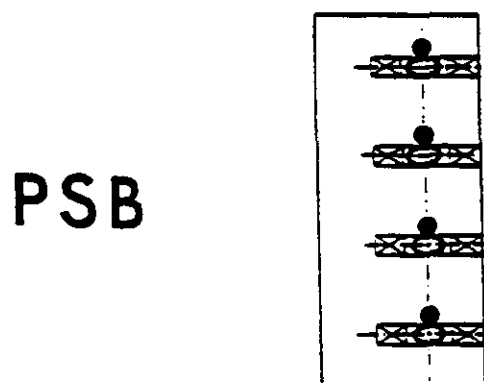
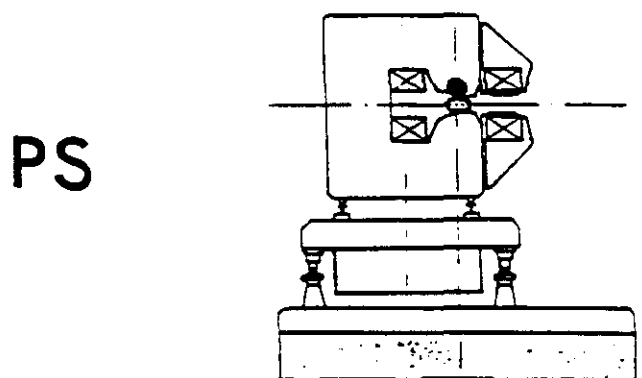


FIG.1

● Dosimeter position

Integrated doses in 1998 in the PS-Booster

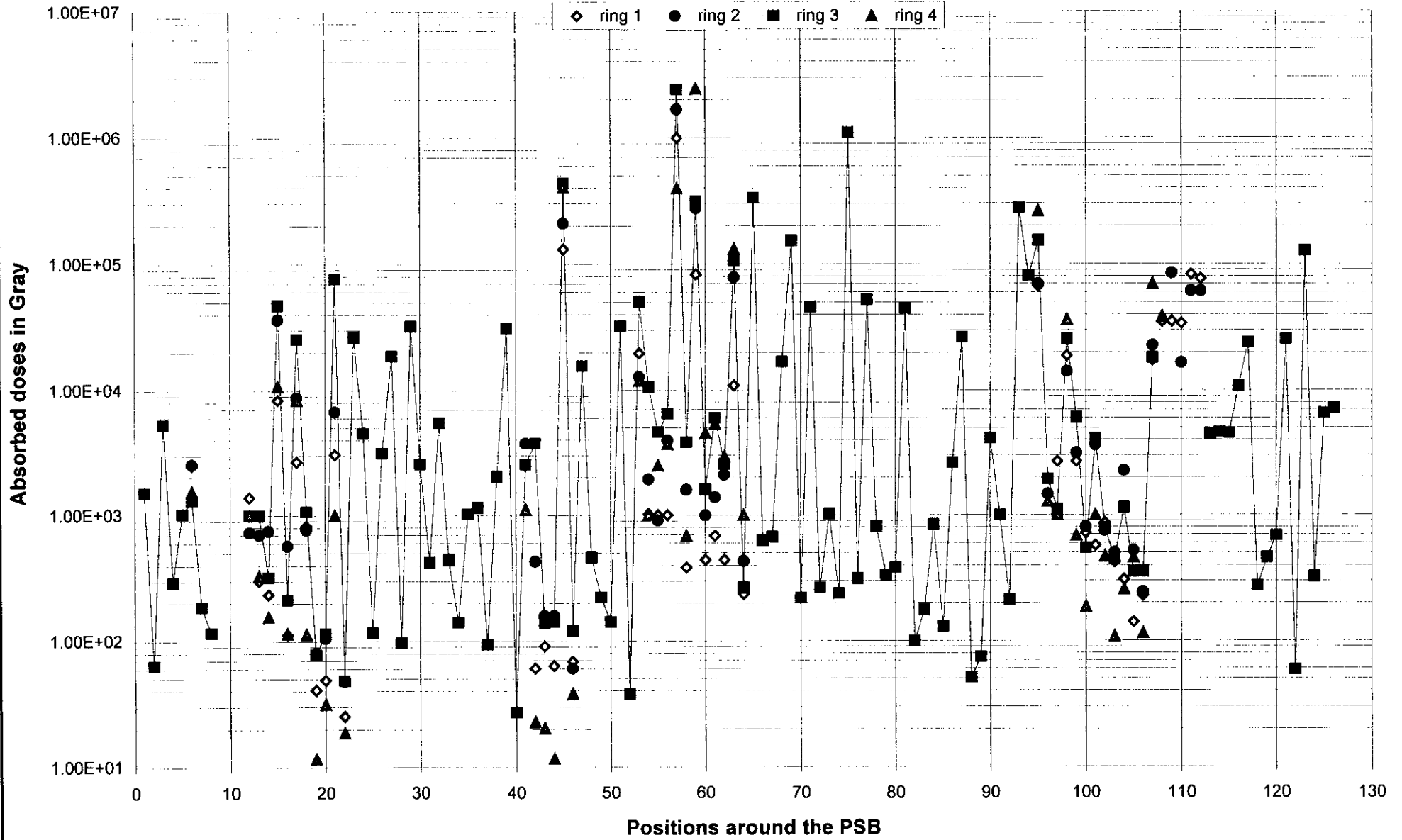


Fig. 2a

Integrated doses from 1975 to 1998 in the PS-Booster

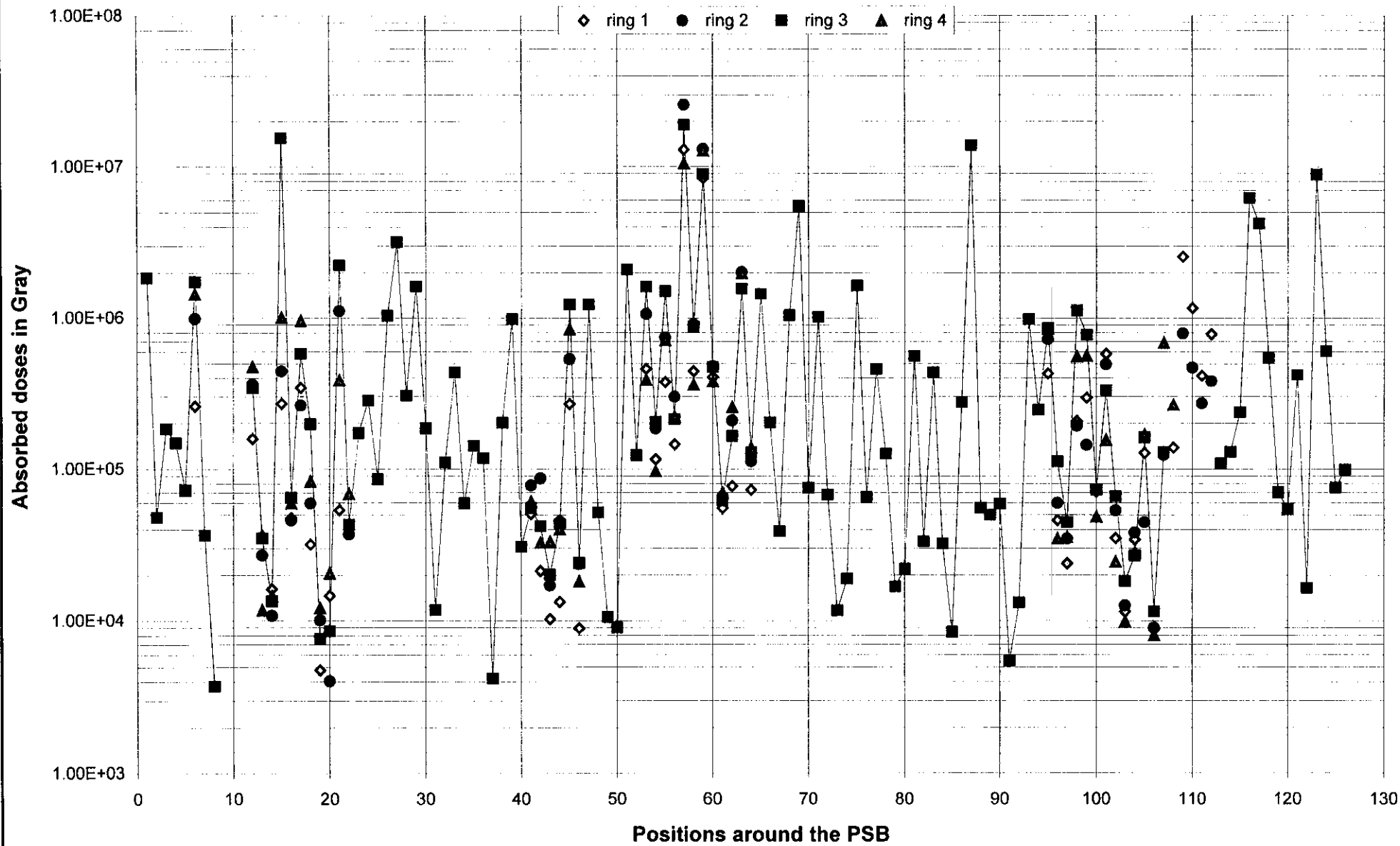
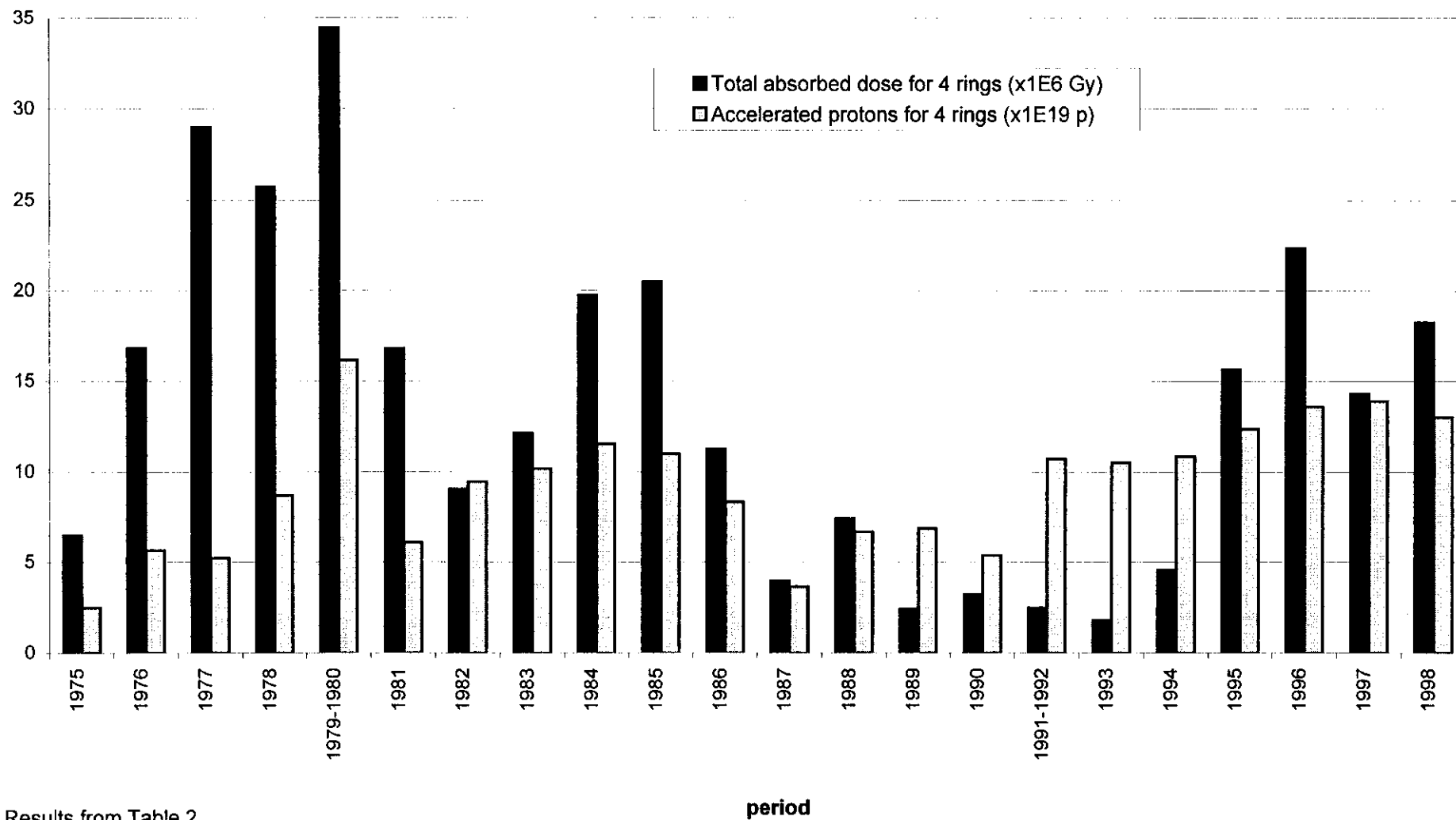


Fig. 2b

Booster - Total absorbed dose and number of accelerated protons evolution over 4 rings from 1975 to 1998



Results from Table 2

Fig. 3

**Booster - Average intensity and dose per accelerated proton evolution over 4 rings
from 1975 to 1998**

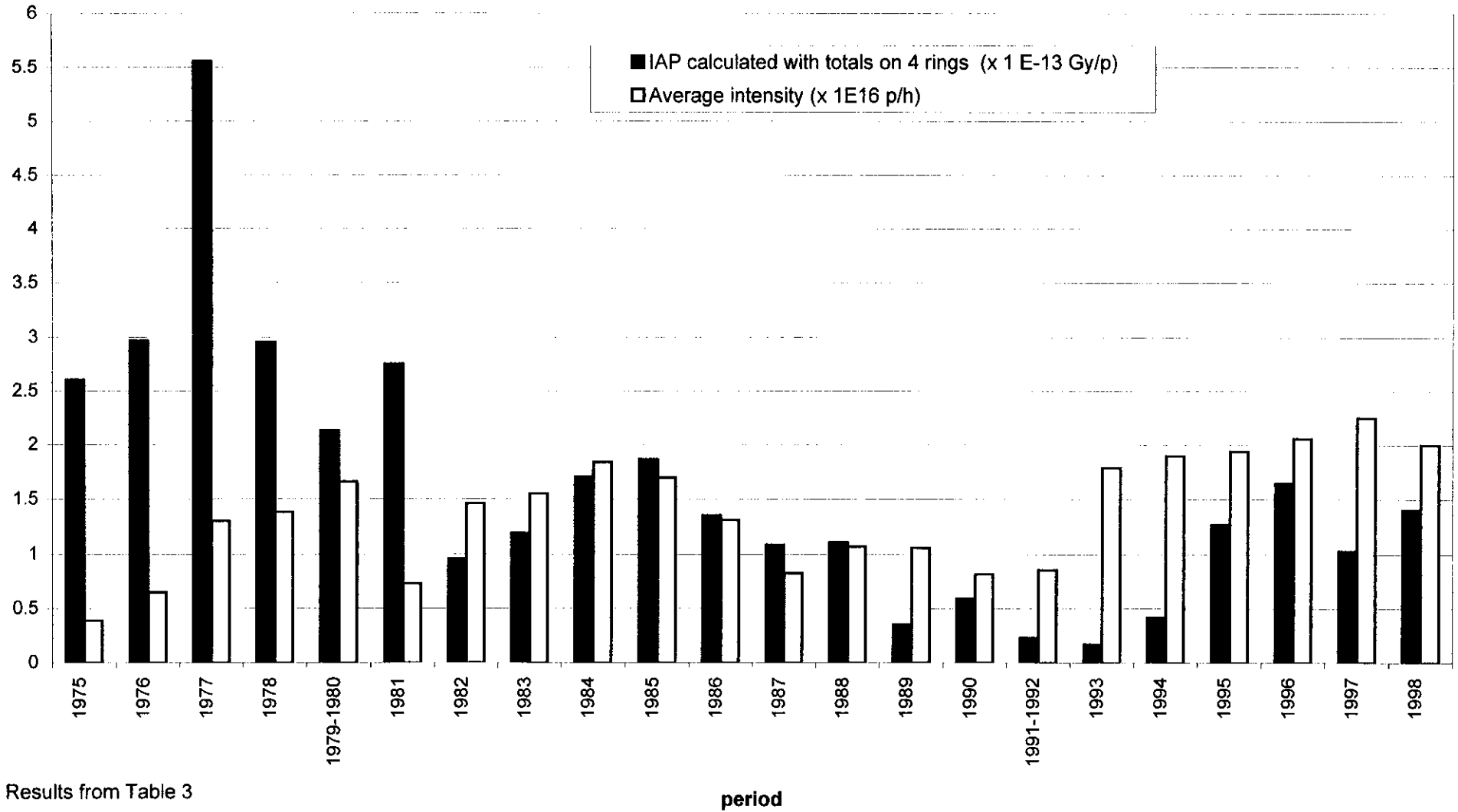
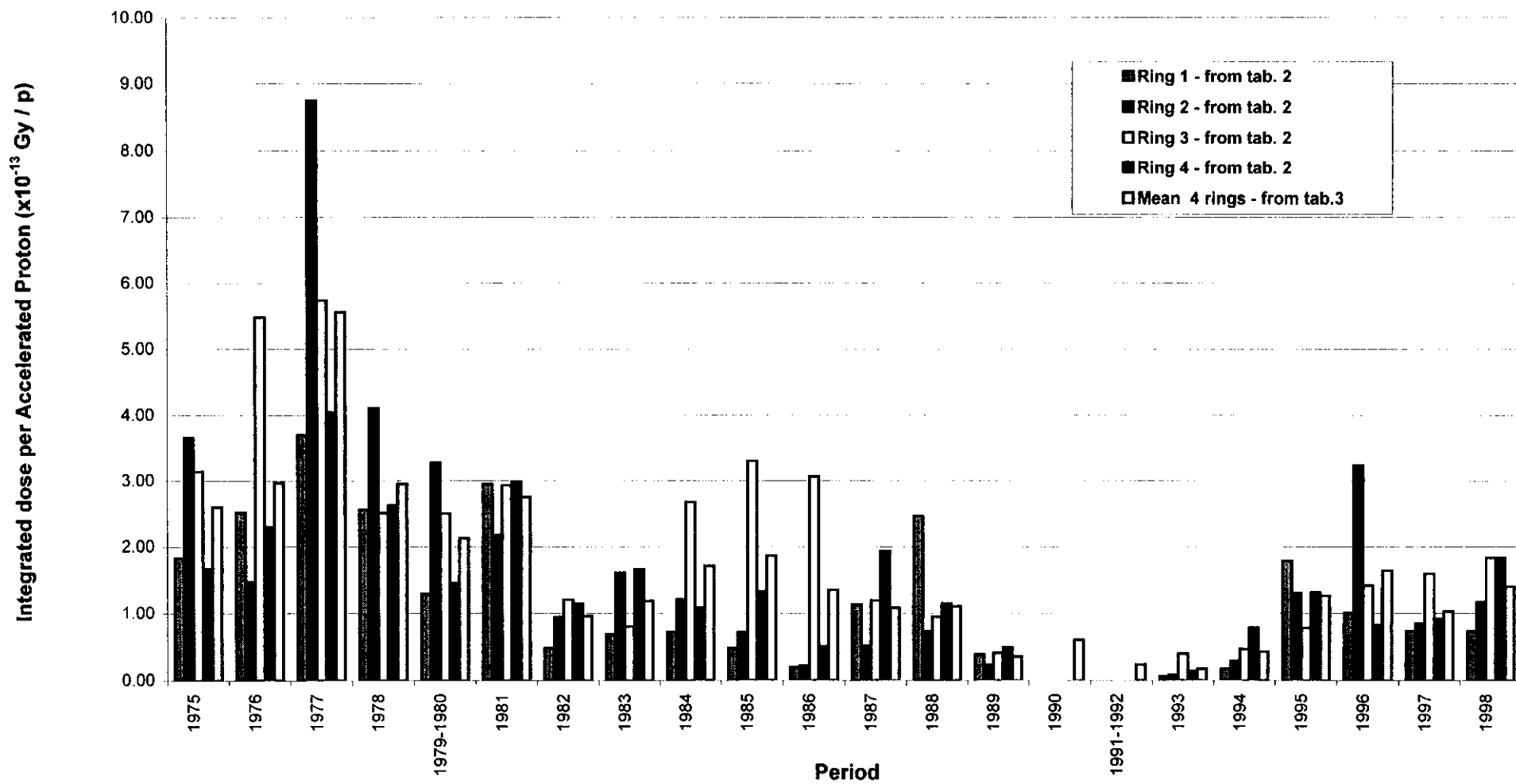


Fig. 4

**Integrated dose by Accelerated Proton (IAP) in Booster:
evolution from 1975**



Results from Tables 2 and 3.

Fig. 5

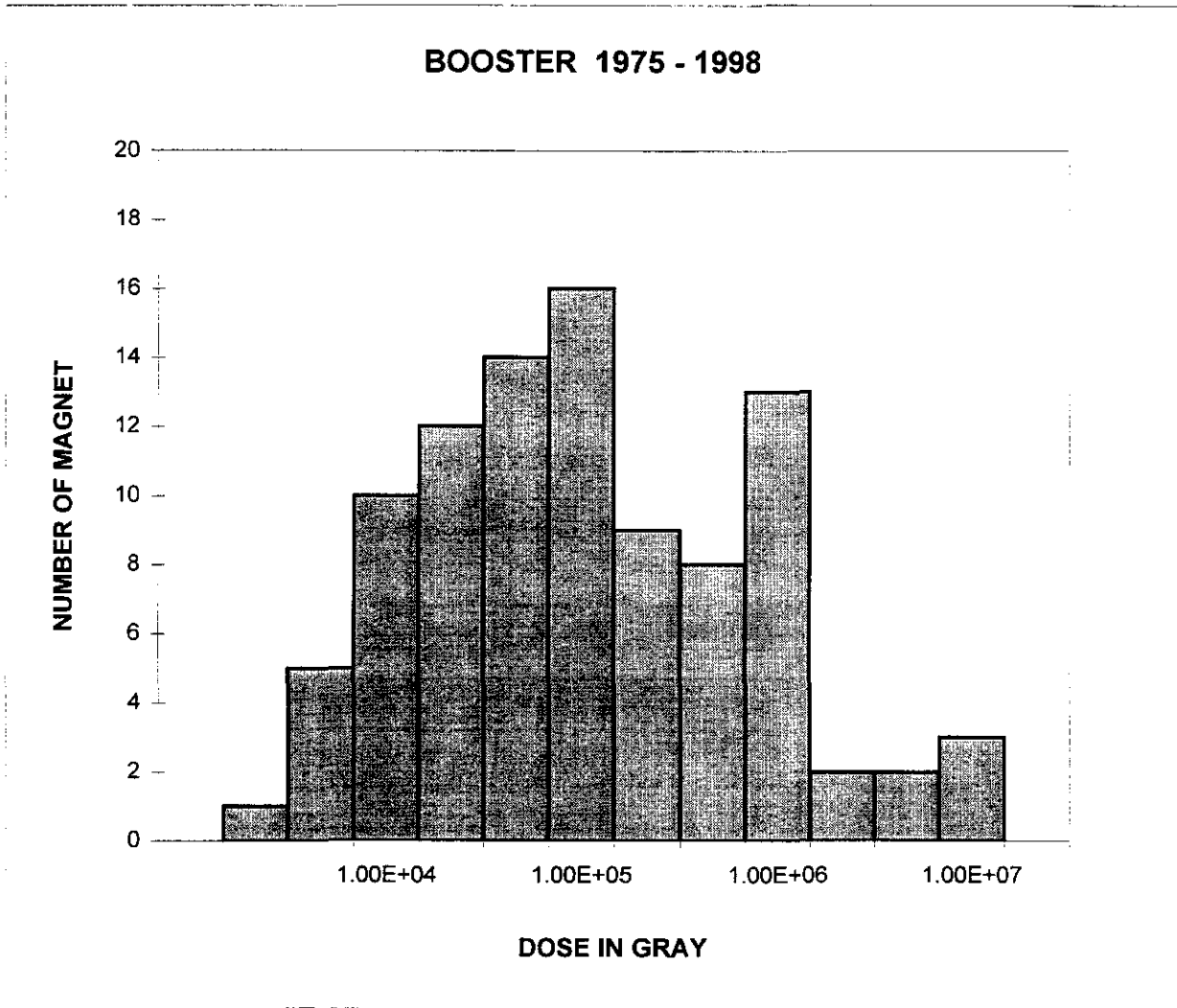
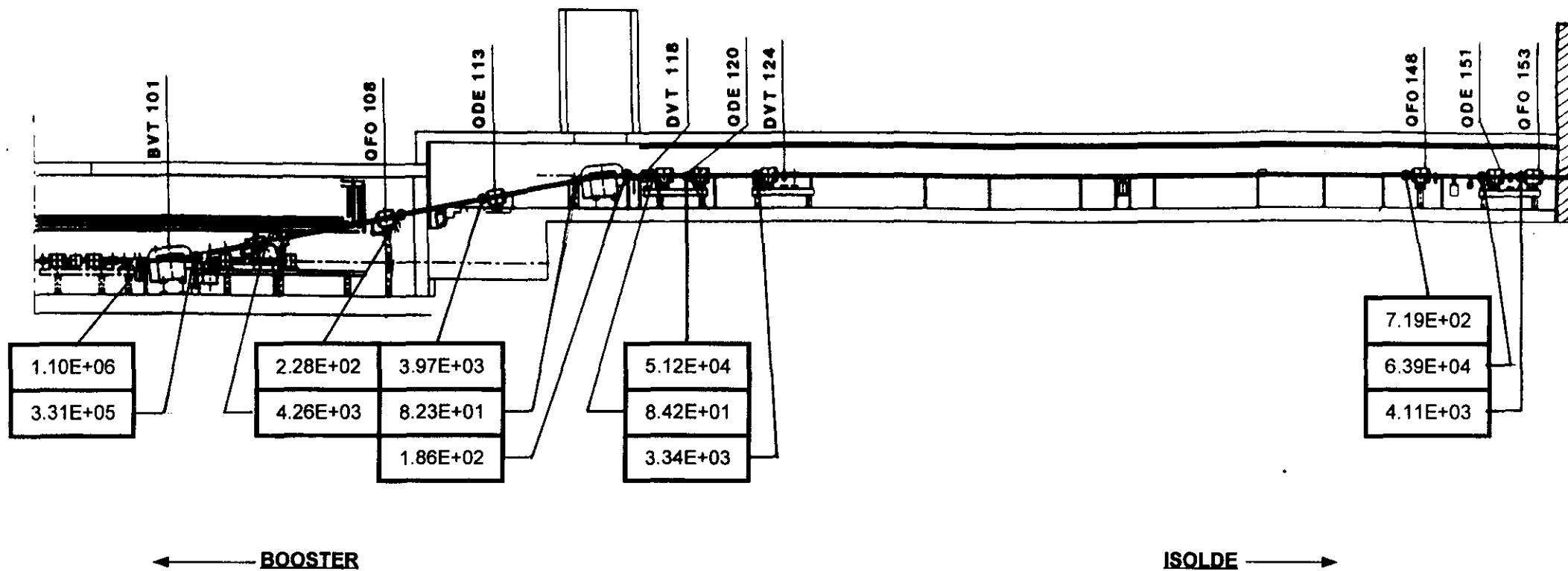


Fig. 6 Dose range distribution to the 95 PSB magnet coils in ring 3 for the period 1975 to 1998

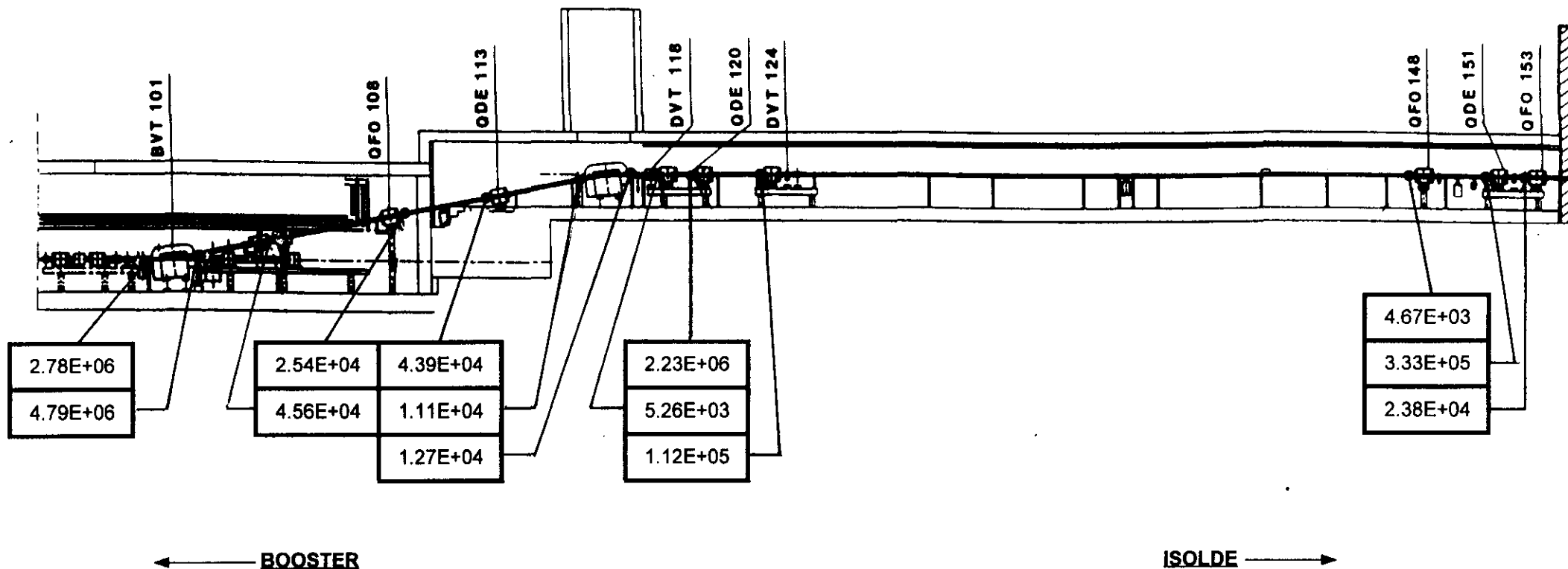


Transfer line BOOSTER - ISOLDE

INTEGRATED DOSES IN GRAY

in 1998.

Fig. 7a



Transfer line BOOSTER - ISOLDE

INTEGRATED DOSES IN GRAY

from February 1993 to December 1998

Fig. 7b

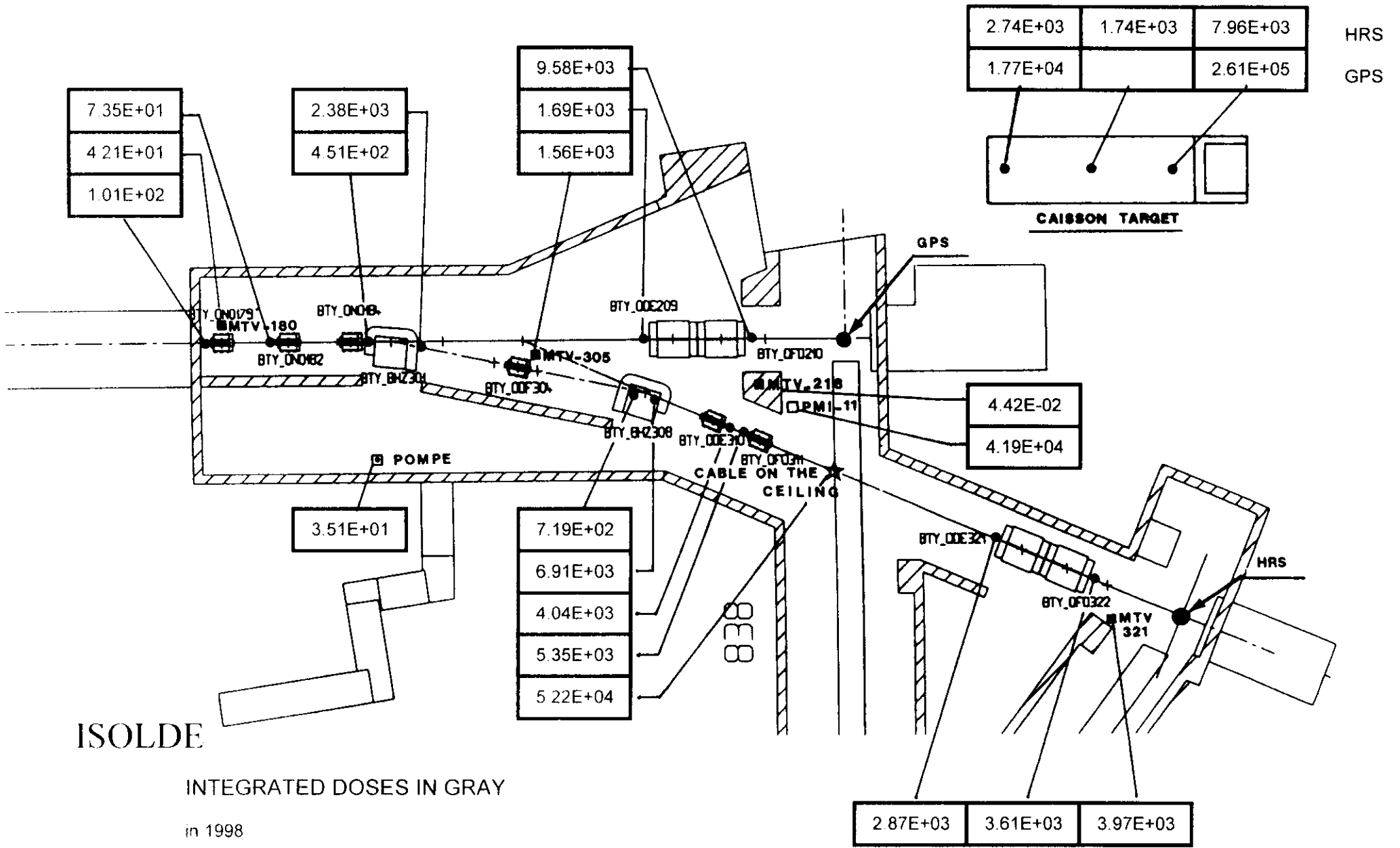
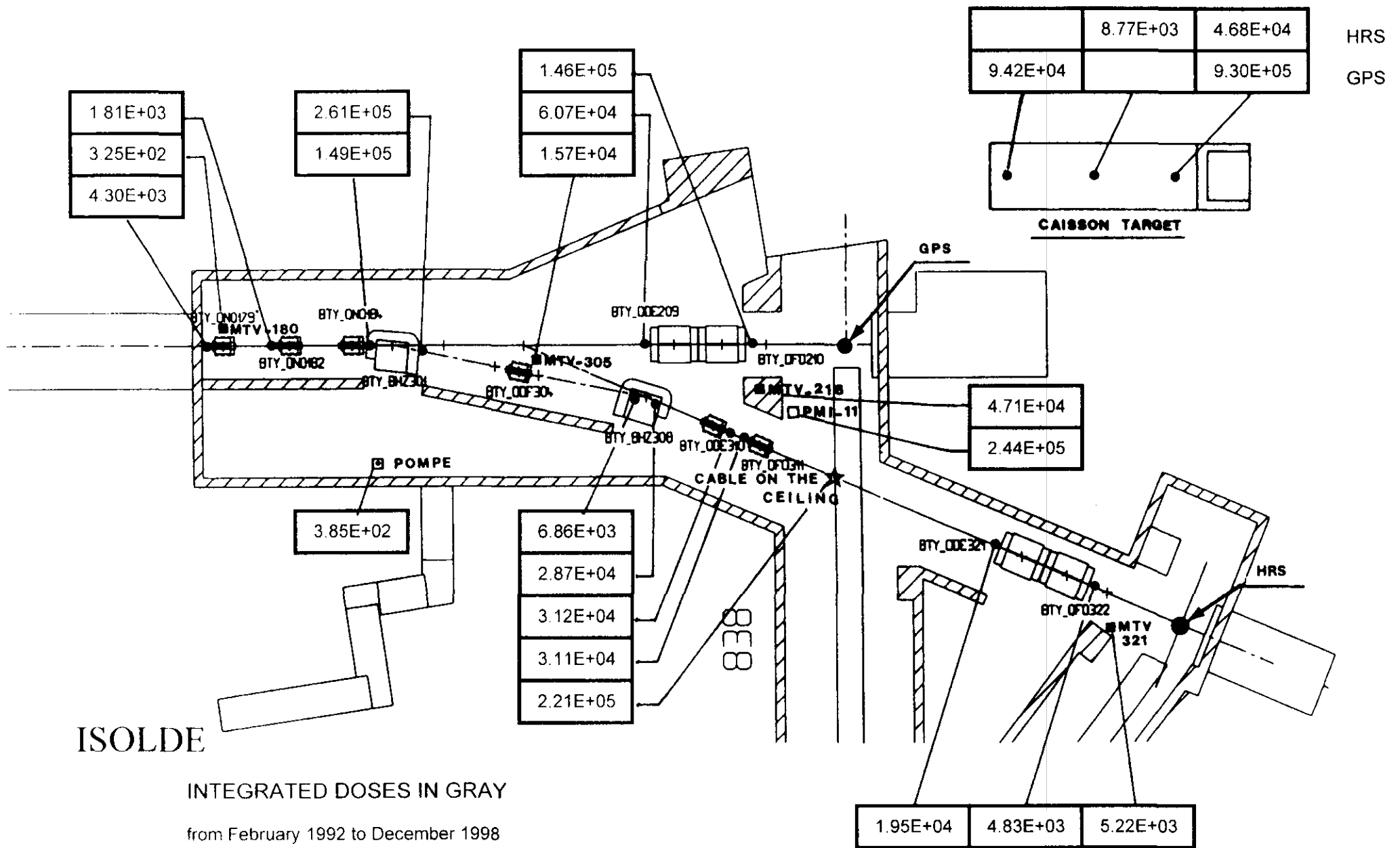


Fig. 8a



Proton Synchrotron
Integrated doses from March to December 1998

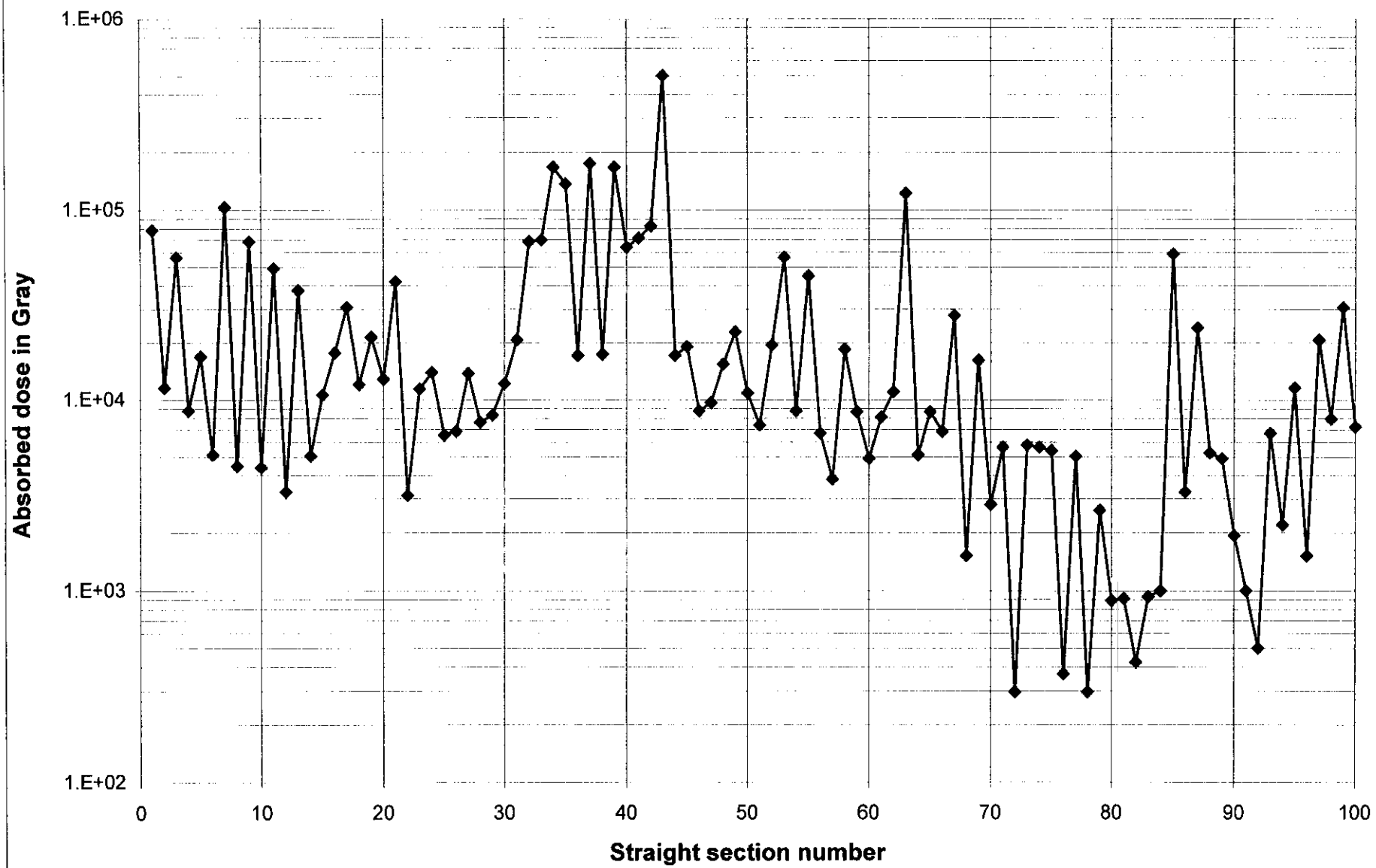


Fig. 9a

Proton Synchrotron Integrated doses from 1966 to 1998

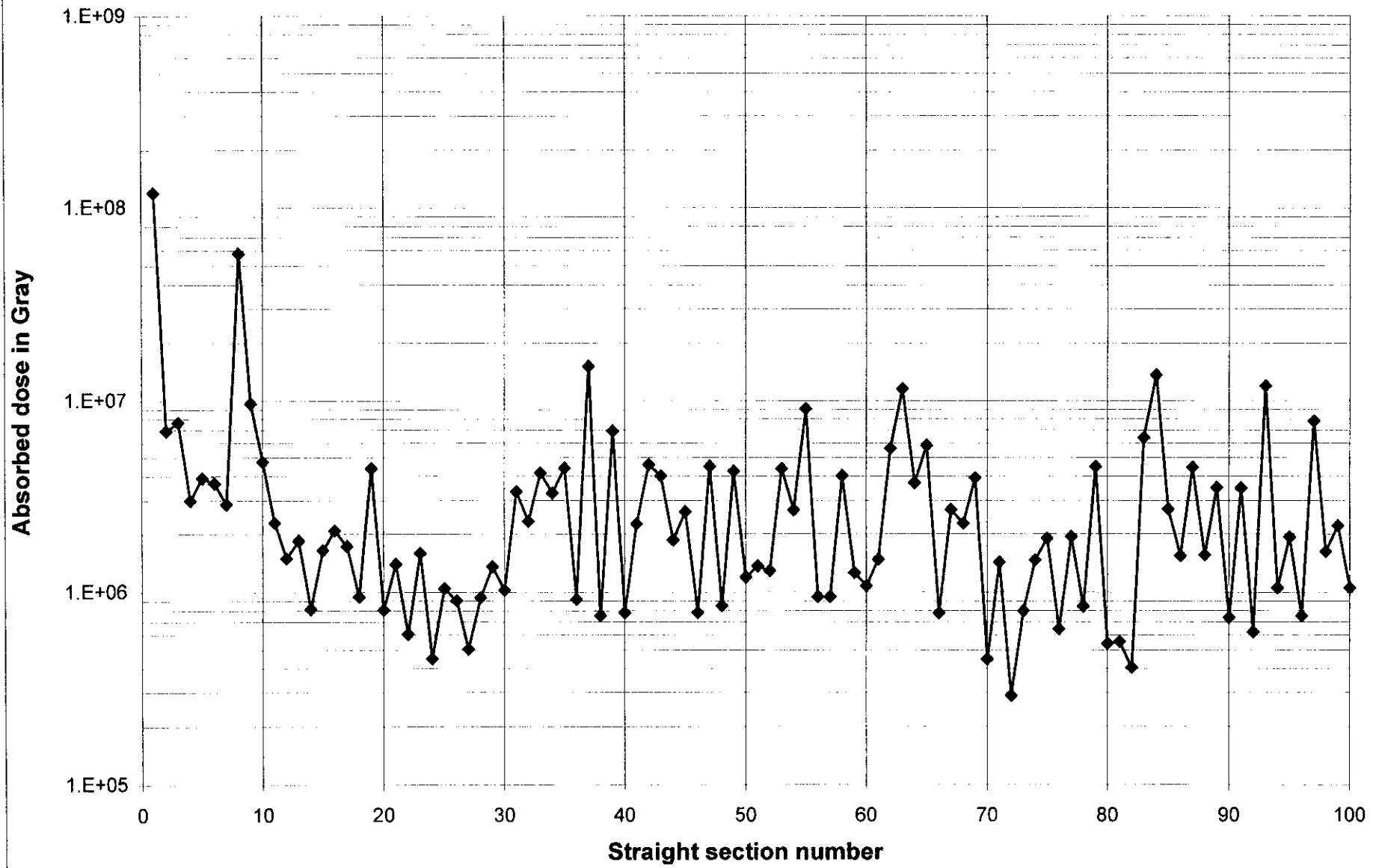
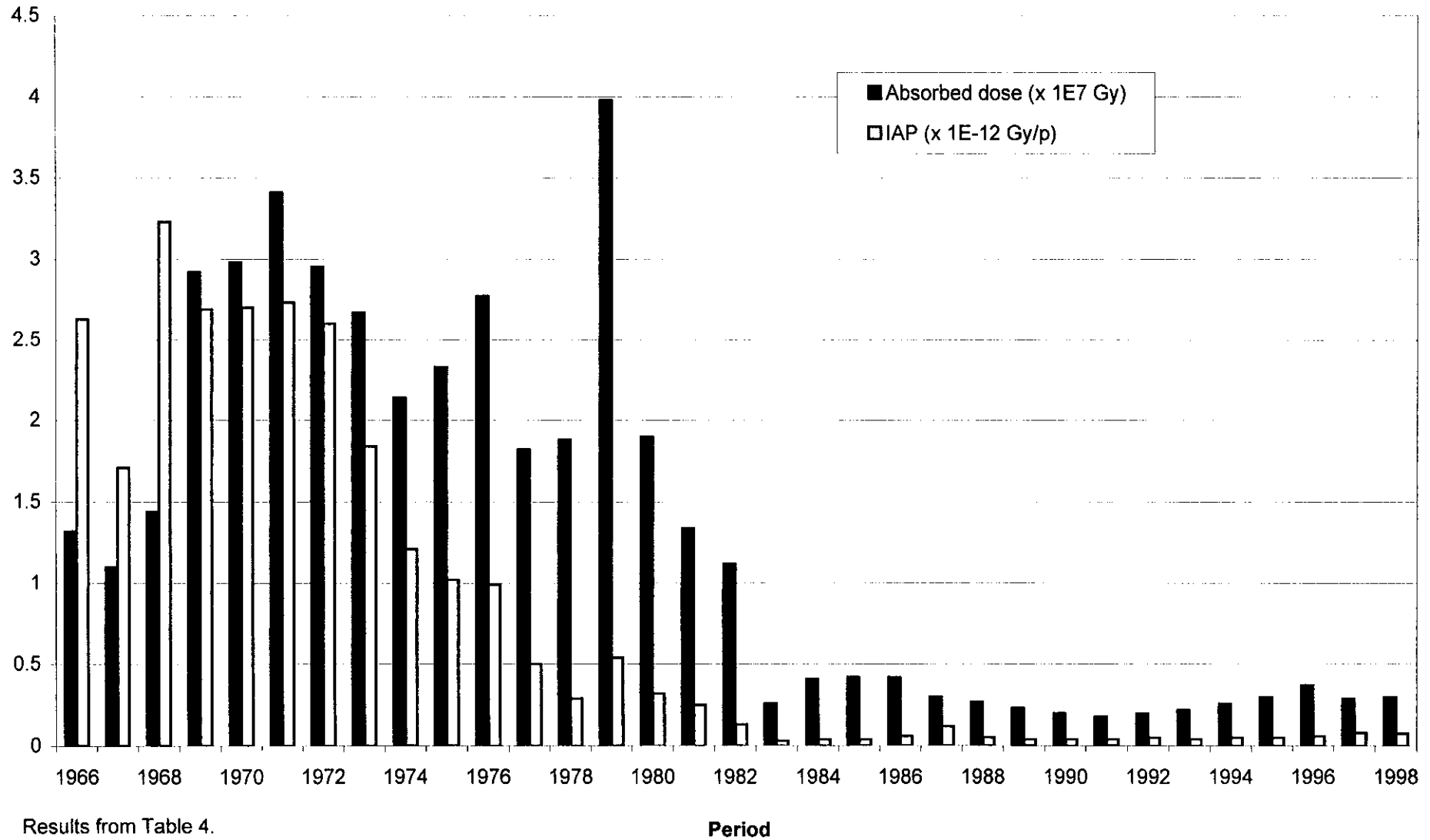


Fig. 9b

Doses and Integrated doses per Accelerated proton (IAP) in the PS: evolution from 1966.



Results from Table 4.

Fig. 10

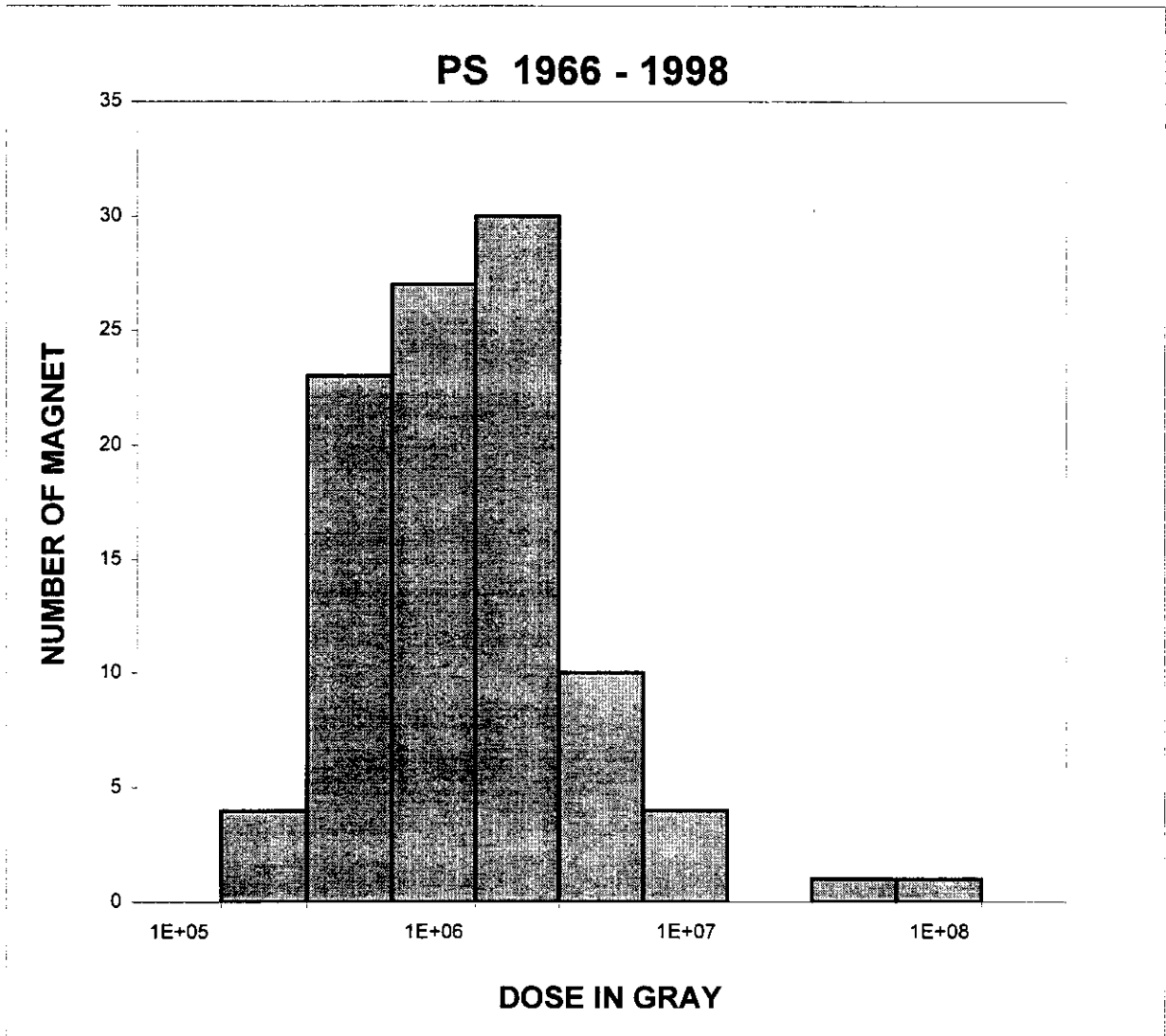


Fig. 11 Dose range distribution to the 100 PS magnet coils for the period 1966 - 1998

LIL - TARGET AREA

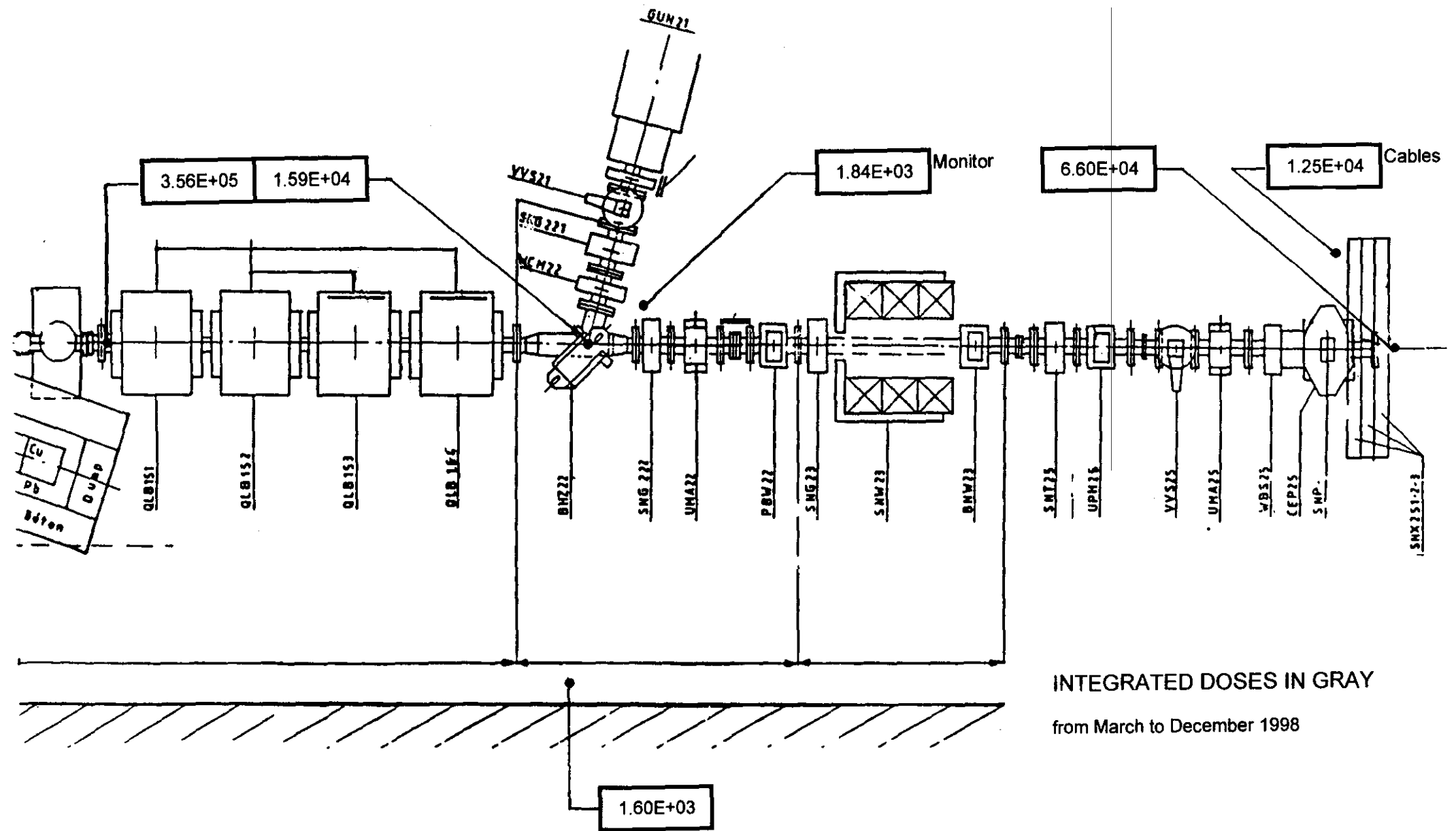


Fig. 12 a

LIL - TARGET AREA

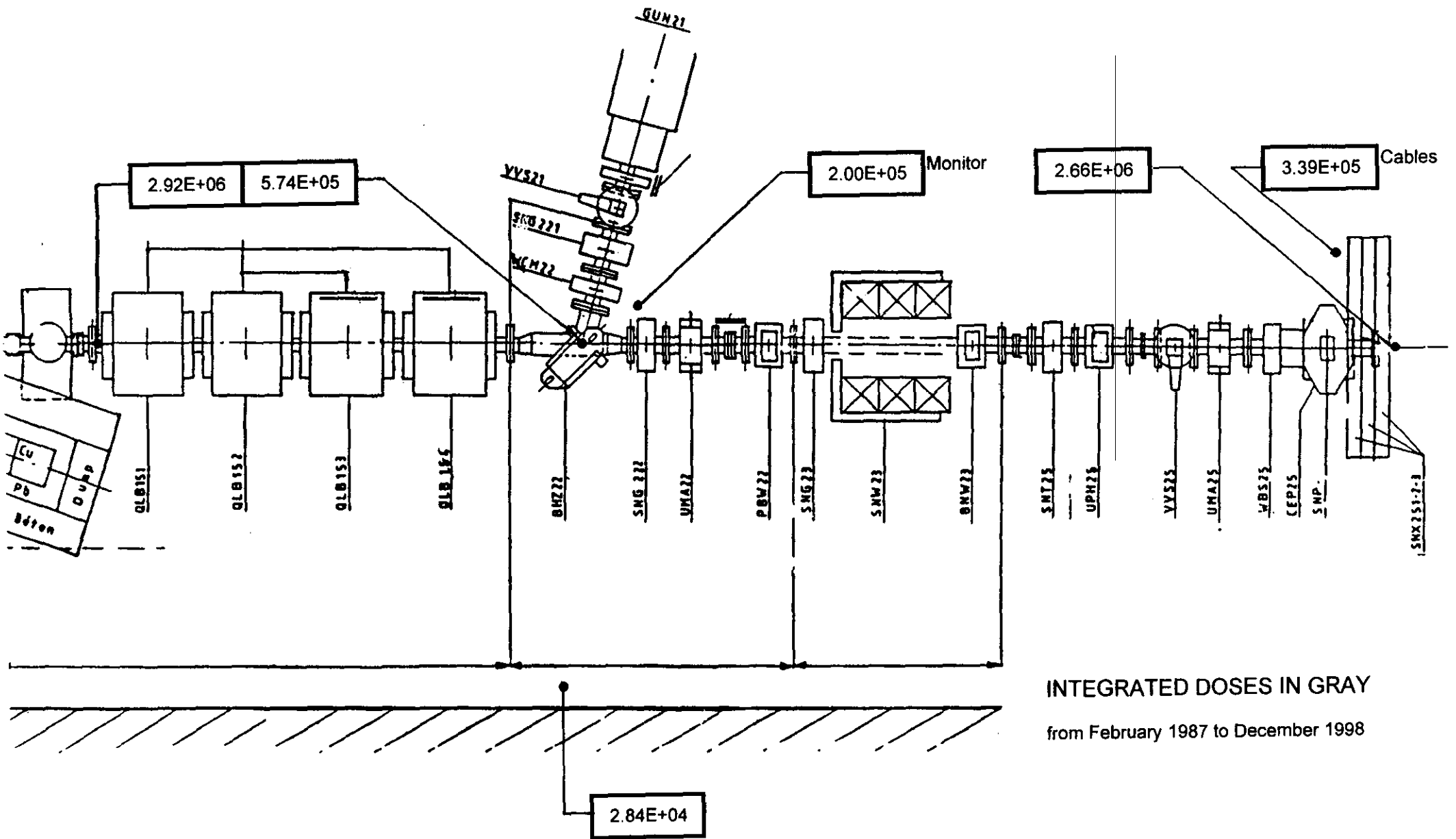
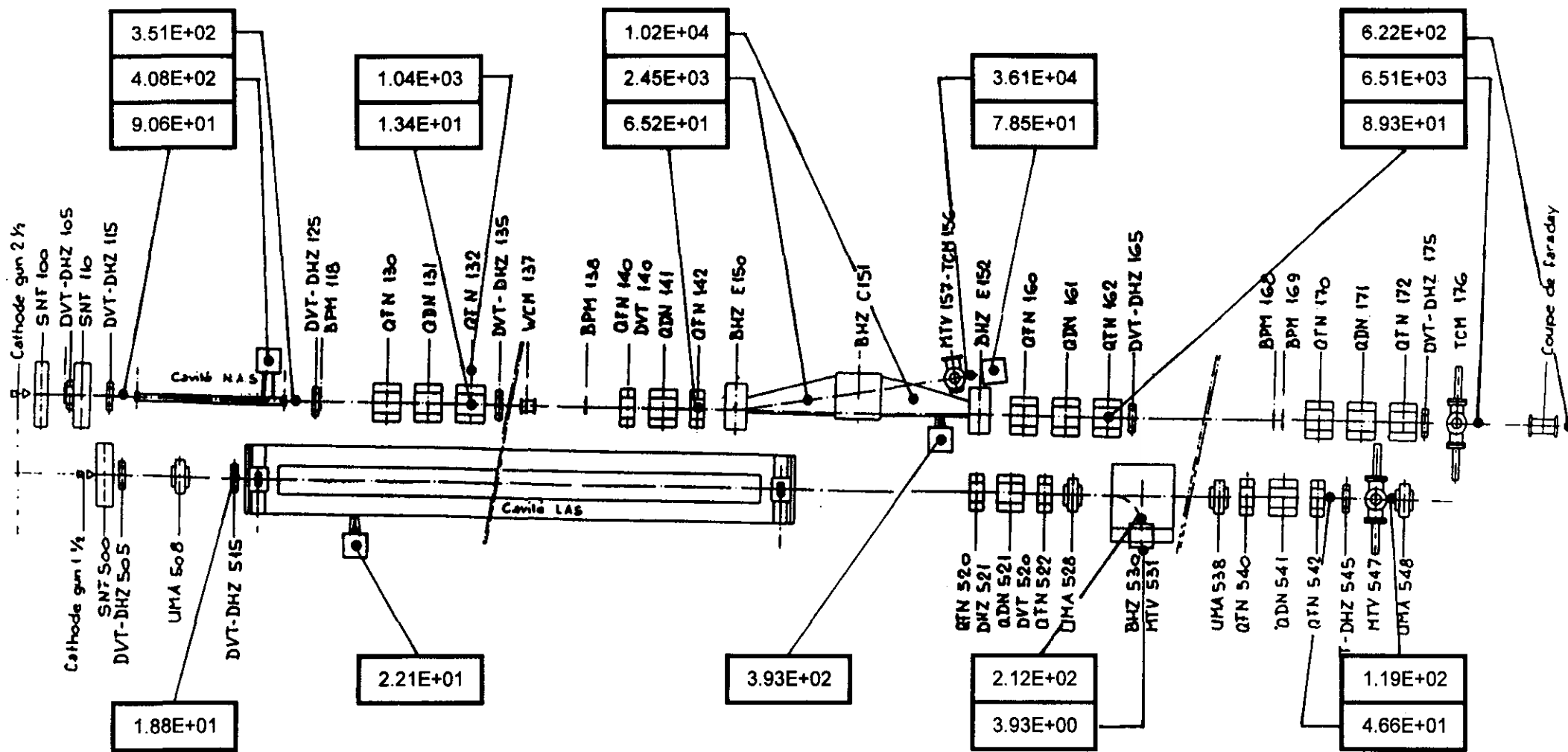


Fig. 12 b

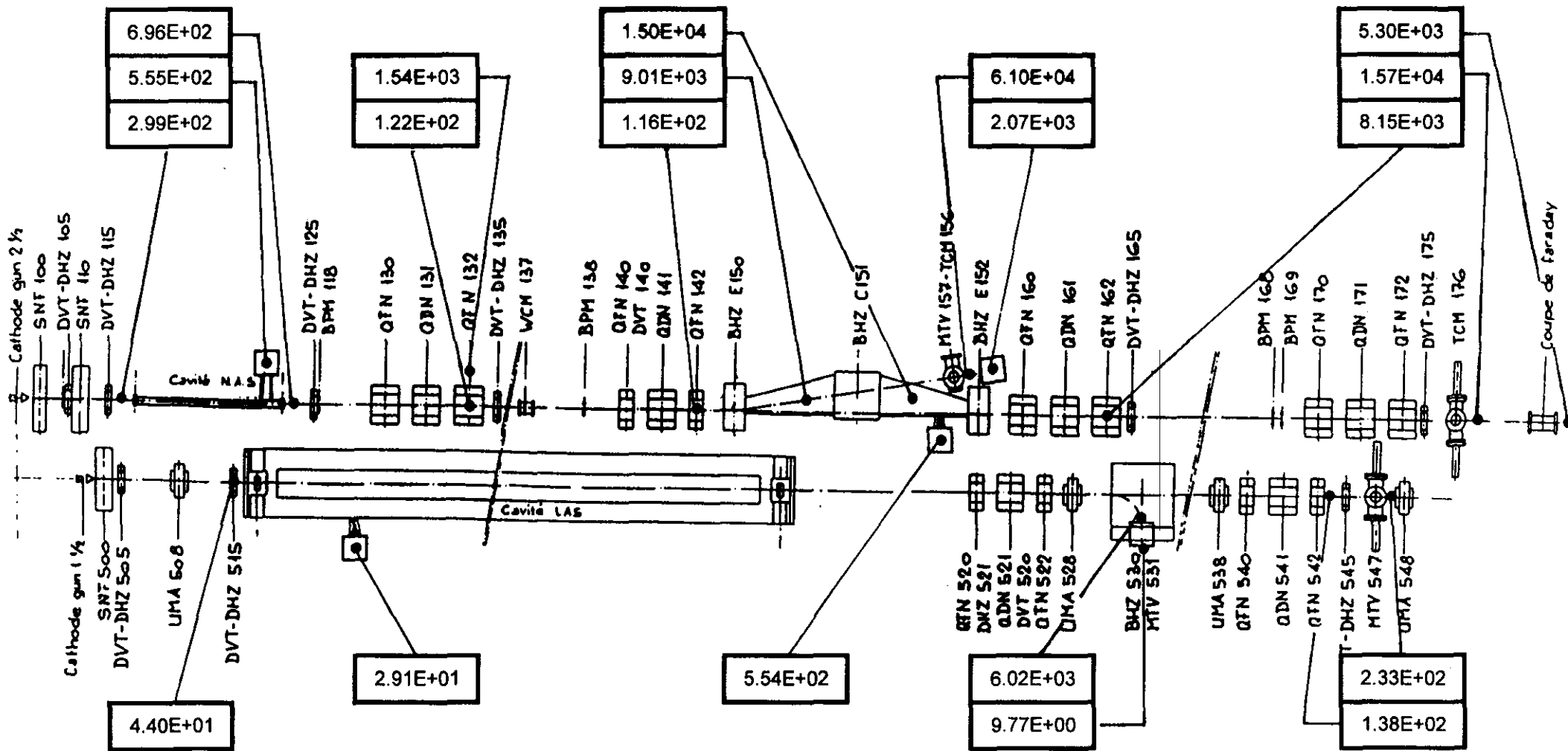


CLIC TEST FACILITY

INTEGRATED DOSES IN GRAY

in 1998.

Fig. 13 a



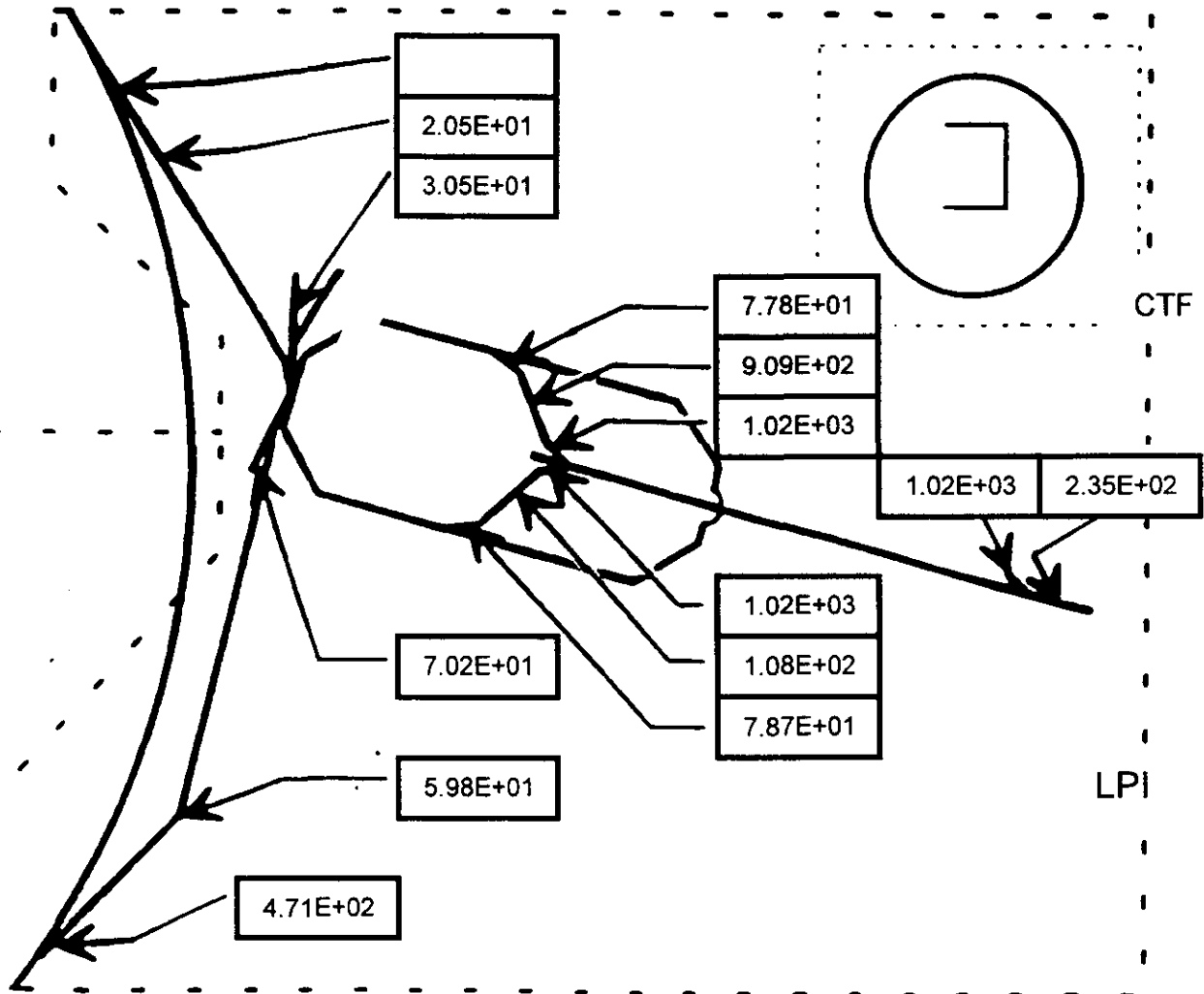
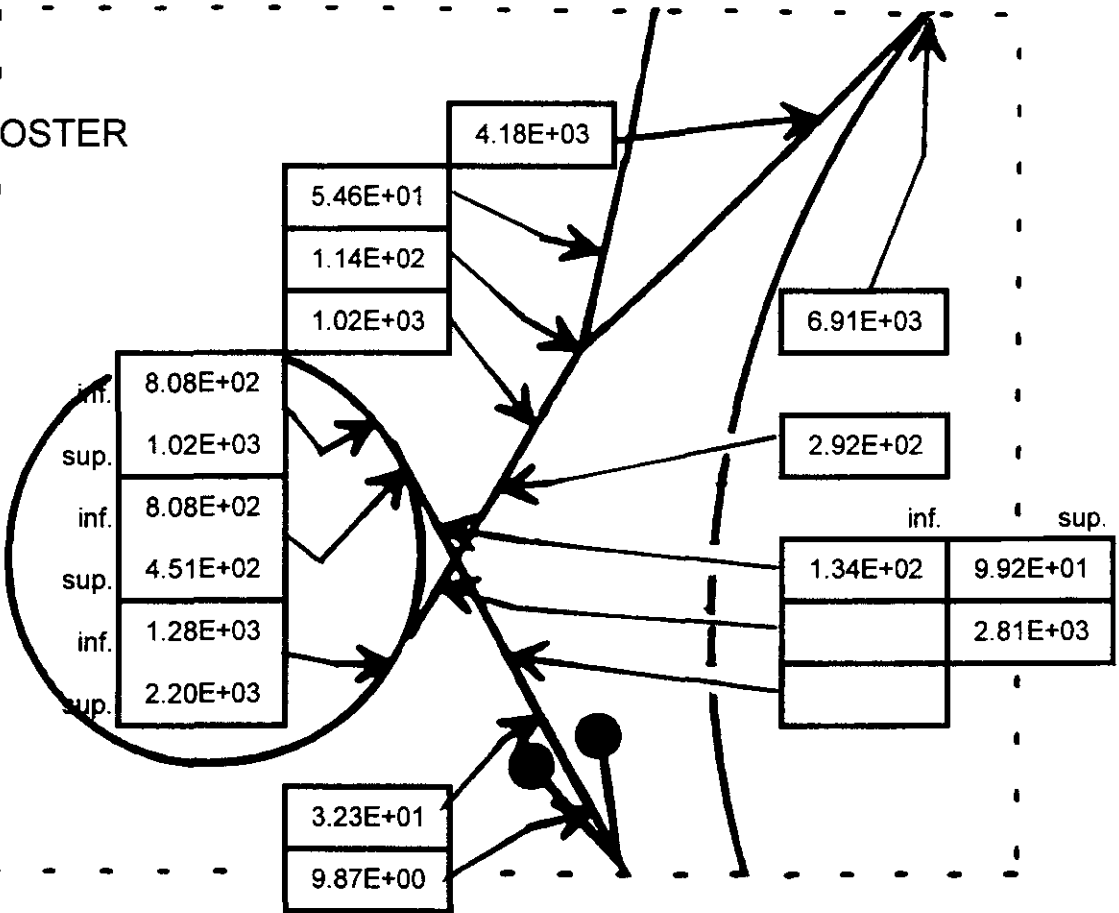
CLIC TEST FACILITY

INTEGRATED DOSES IN GRAY

from October 1996 to December 1998

Fig. 13 b

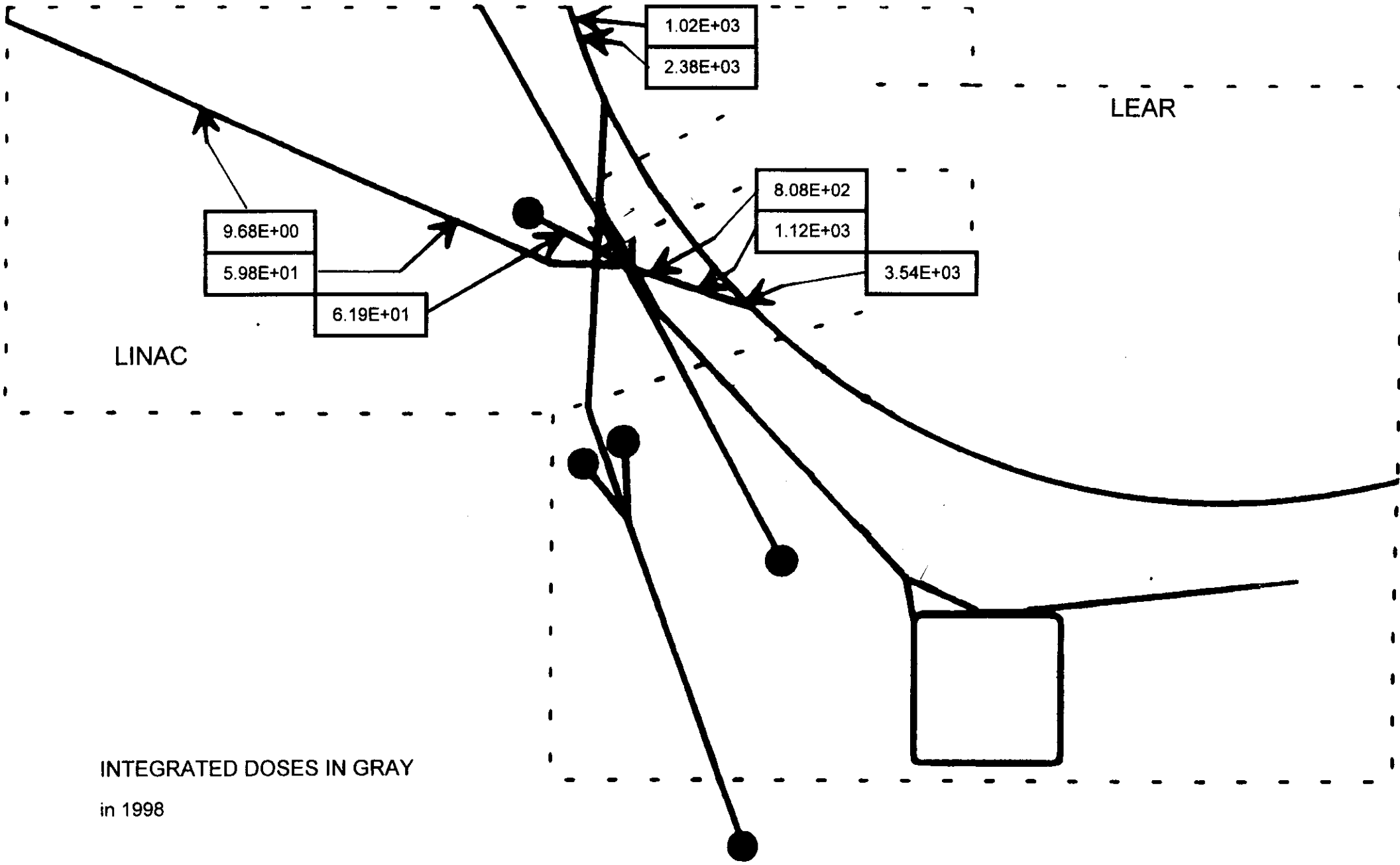
BOOSTER



INTEGRATED DOSES IN GRAY

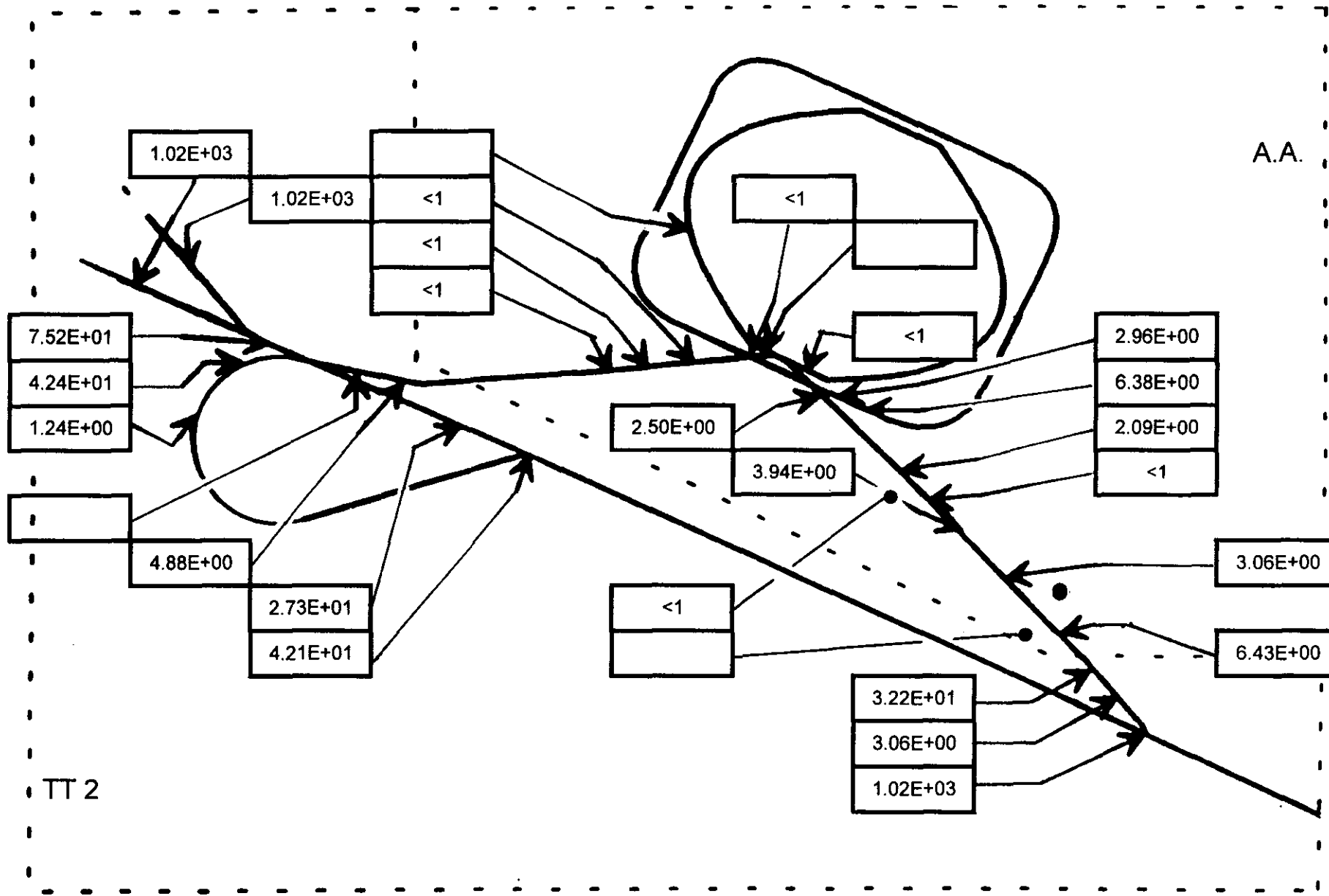
Fig. 14

in 1998.



INTEGRATED DOSES IN GRAY
in 1998

Fig. 15



INTEGRATED DOSES IN GRAY

in 1998

Fig. 16

ISOLDE

INTEGRATED DOSE IN GRAY

in 1998

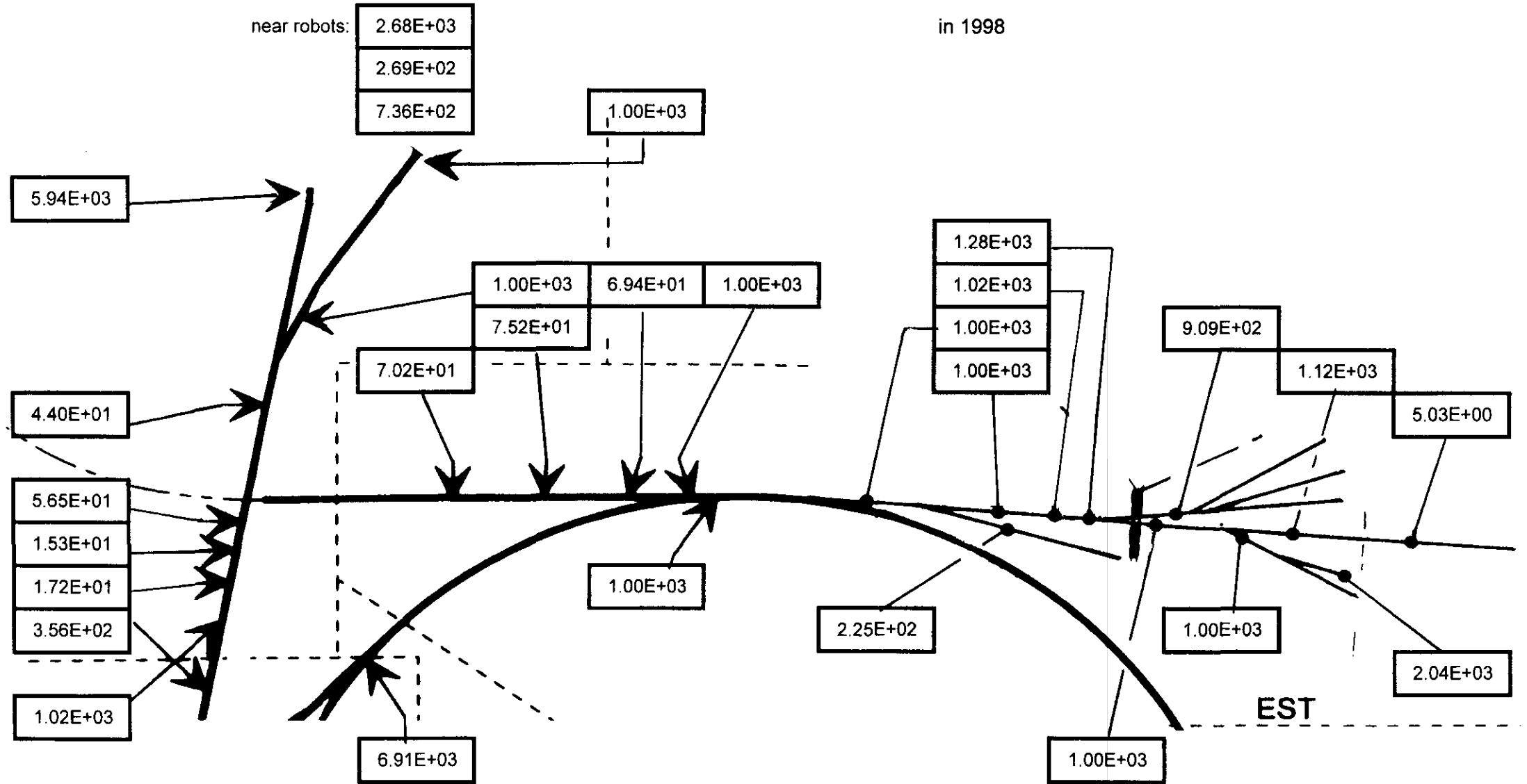


Fig. 17

APPENDIX I

NOMENCLATURE OF THE POSITIONS IN THE BOOSTER

Number -----	Position -----	Number -----	Position -----
1	BI. QNO30	21	BR1. BHZ22U
2	BI. QNO40	21	BR2. BHZ22U
3	BI3. -DISU	21	BR3. BHZ22U
4	BI3. -DISD	21	BR4. BHZ22U
5	BI3. SMVU	22	BR1. BHZ22D
6	BI1. SMVD	22	BR2. BHZ22D
6	BI2. SMVD	22	BR3. BHZ22D
6	BI3. SMVD	22	BR4. BHZ22D
6	BI4. SMVD	23	BR3. BHZ31U
7	BI3. QNO50U	24	BR3. BHZ31D
8	BI3. QNO60U	25	BR3. QDE3U
12	BR1. BHZ11D	26	BR3. QFO32U
12	BR2. BHZ11D	27	BR3. BHZ32U
12	BR3. BHZ11D	28	BR3. BHZ32D
12	BR4. BHZ11D	29	BR3. BHZ41U
13	BR1. QDE1U	30	BR3. BHZ41D
13	BR2. QDE1U	31	BR3. QDE4U
13	BR3. QDE1U	32	BR3. QFO42U
13	BR4. QDE1U	33	BR3. BHZ42U
14	BR1. QFO12U	34	BR3. BHZ42D
14	BR2. QFO12U	35	BR3. BHZ51U
14	BR3. QFO12U	36	BR3. BHZ51D
14	BR4. QFO12U	37	BR3. QDE5U
15	BR1. BHZ12U	38	BR3. QFO52U
15	BR2. BHZ12U	39	BR3. BHZ52U
15	BR3. BHZ12U	40	BR3. BHZ52D
15	BR4. BHZ12U	41	BR1. BHZ61U
16	BR1. BHZ12D	41	BR2. BHZ61U
16	BR2. BHZ12D	41	BR3. BHZ61U
16	BR3. BHZ12D	41	BR4. BHZ61U
16	BR3. BHZ12D	42	BR1. BHZ61D
16	BR4. BHZ12D	42	BR2. BHZ61D
17	BR1. BHZ21U	42	BR3. BHZ61D
17	BR2. BHZ21U	42	BR4. BHZ61D
17	BR3. BHZ21U	43	BR1. QDE6U
17	BR4. BHZ21U	43	BR2. QDE6U
18	BR1. BHZ21D	43	BR3. QDE6U
18	BR2. BHZ21D	43	BR4. QDE6U
18	BR3. BHZ21D	44	BR1. QFO62U
18	BR4. BHZ21D	44	BR2. QFO62U
19	BR1. QDE2U	44	BR3. QFO62U
19	BR2. QDE2U	44	BR4. QFO62U
19	BR3. QDE2U	45	BR1. BHZ62U
19	BR4. QDE2U	45	BR2. BHZ62U
20	BR1. QFO22U	45	BR3. BHZ62U
20	BR2. QFO22U	45	BR4. BHZ62U
20	BR3. QFO22U	46	BR1. BHZ62D
20	BR4. QFO22U	46	BR2. BHZ62D

Number	Position	Number	Position
46	BR3.BHZ62D	63	BR2.BHZ92U
46	BR4.BHZ62D	63	BR3.BHZ92U
47	BR3.BHZ71U	63	BR4.BHZ92U
48	BR3.BHZ71D	64	BR1.BHZ92D
49	BR3.QDE7U	64	BR2.BHZ92D
50	BR3.QFO72U	64	BR3.BHZ92D
51	BR3.BHZ72U	64	BR4.BHZ92D
52	BR3.BHZ72D	65	BR3.BHZ101U
53	BR1.BHZ81U	66	BR3.BHZ101D
53	BR2.BHZ81U	67	BR3.QDE10U
53	BR3.BHZ81U	68	BR3.QFO102U
53	BR4.BHZ81U	69	BR3.BHZ102U
54	BR1.BHZ81D	70	BR3.BHZ102D
54	BR2.BHZ81D	71	BR3.BHZ111U
54	BR3.BHZ81D	72	BR3.BHZ111D
54	BR4.BHZ81D	73	BR3.QDE11U
55	BR1.QDE8U	74	BR3.QFO112U
55	BR2.QDE8U	75	BR3.BHZ112U
55	BR3.QDE8U	76	BR3.BHZ112D
55	BR4.QDE8U	77	BR3.BHZ121U
56	BR1.QFO82U	78	BR3.BHZ121D
56	BR2.QFO82U	79	BR3.QDE12U
56	BR3.QFO82U	80	BR3.QFO122U
56	BR4.QFO82U	81	BR3.BHZ122U
57	BR1.BHZ82U	82	BR3.BHZ122D
57	BR2.BHZ82U	83	BR3.BHZ131U
57	BR3.BHZ82U	84	BR3.BHZ131D
57	BR4.BHZ82U	85	BR3.QDE13U
58	BR1.BHZ82D	86	BR3.QFO132U
58	BR2.BHZ82D	87	BR3.BHZ132U
58	BR3.BHZ82D	88	BR3.BHZ132D
58	BR4.BHZ82D	89	BR3.BHZ141U
59	BR1.BHZ91U	90	BR3.BHZ141D
59	BR2.BHZ91U	91	BR3.QDE14U
59	BR3.BHZ91U	92	BR3.QFO142U
59	BR4.BHZ91U	93	BR3.BHZ142U
60	BR1.BHZ91D	94	BR3.BHZ142D
60	BR2.BHZ91D	95	BR1.BHZ151U
60	BR3.BHZ91D	95	BR2.BHZ151U
60	BR4.BHZ91D	95	BR3.BHZ151U
61	BR1.QDE9U	95	BR4.BHZ151U
61	BR2.QDE9U	96	BR1.QFO151U
61	BR3.QDE9U	96	BR2.QFO151U
61	BR4.QDE9U	96	BR3.QFO151U
62	BR1.QFO92U	96	BR4.QFO151U
62	BR2.QFO92U	97	BR1.QDE15U
62	BR3.QFO92U	97	BR2.QDE15U
62	BR4.QFO92U	97	BR3.QDE15U
63	BR1.BHZ92U	97	BR4.QDE15U

Number	Position	Number	Position
98	BR1.QFO152U	105	BR4.BHZ162U
98	BR2.QFO152U	106	BR1.BHZ162D
98	BR3.QFO152U	106	BR2.BHZ162D
98	BR4.QFO152U	106	BR3.BHZ162D
99	BR1.BHZ152U	106	BR4.BHZ162D
99	BR2.BHZ152U	107	BT1.BVT10
99	BR3.BHZ152U	107	BT2.DVT10
99	BR4.BHZ152U	107	BT3.DVT10
100	BR1.BHZ151D	107	BT4.BVT10
100	BR2.BHZ151D	108	BT1.SMV10U
100	BR3.BHZ151D	109	BT1.QNO10U
100	BR4.BHZ151D	109	BT2.QNO10U
101	BR1.BHZ161U	110	BT1.QNO10D
101	BR2.BHZ161U	110	BT2.QNO10D
101	BR3.BHZ161U	111	BT1.QNO20U
101	BR4.BHZ161U	111	BT2.QNO20U
102	BR1.BHZ161D	112	BT1.QNO20D
102	BR2.BHZ161D	112	BT2.QNO20D
102	BR3.BHZ161D	113	BT.BVT20U
102	BR4.BHZ161D	114	BT.DVT30U
103	BR1.QDE16U	115	BT.SMV20U
103	BR2.QDE16U	116	BT.SMV20D
103	BR3.QDE16U	117	BT.QNO30D
103	BR4.QDE16U	118	BT.KFA20U
104	BR1.QFO162U	119	BT.KFA20D
104	BR2.QFO162U	120	BT.QNO50U
104	BR3.QFO162U	121	BT.BHZ10U
104	BR4.QFO162U	122	BT.BHZ10D
105	BR1.BHZ162U	123	BTM.BHZ10U
105	BR2.BHZ162U	124	BTM.BHZ10D
105	BR3.BHZ162U	125	BTM.QNO20